Investigating the pathogenicity of missense mutations in *VSX1* and their association with corneal dystrophies

by

Anastasia Marie Litke
Bachelor of Science, University of Victoria, 2015

A Thesis Submitted in Partial Fulfillment
of the Requirements for the Degree of

MASTER OF SCIENCE

in the Department of Biology (Neuroscience)

Supervisory Committee

Investigating the pathogenicity of missense mutations in *VSX1* and their association with corneal dystrophies

by

Anastasia Marie Litke
Bachelor of Science, University of Victoria, 2015

Supervisory Committee

Dr. Robert L. Chow, Department of Biology
Supervisor

Dr. Patrick Walter, Department of Biology
Departmental Member

Dr. Leigh Anne Swayne, Division of Medical Sciences
Outside Member

Abstract

Two corneal dystrophies, posterior polymorphous corneal dystrophy (PPCD) and keratoconus, have been associated with missense mutations found in the transcription factor-encoding gene *Visual System Homeobox 1* (*VSX1*). Despite this association, the pathogenic link between *VSX1* and these diseases remains controversial.

To address this issue, I utilized a variety of *in vitro* approaches to study how seven *VSX1* missense mutations found in disease populations that span two highly conserved domains, the homeodomain (HD) and CVC domain affect VSX1 transcriptional activity, protein expression levels and subcellular localization. I also carried out an *in vivo* investigation by generating a mouse line carrying a mutation in *Vsx1*: P254R. Corneal morphology was examined through histology and *ex vivo* whole eye confocal imaging which was used to assess corneal thickness. Quantification of immunocytochemistry was used to characterize terminal marker expression in the inner retina compared to previously described phenotypes in *Vsx1*-null mice.

My *in vitro* results showed that mutations found in both the HD and CVC domain alter the normal transcriptional repression activity in Vsx1. These changes were not due to changes to protein expression or subcellular localization. Characterization of corneal and retinal phenotypes *in vivo* revealed no significant differences in *Vsx1 P254R* mice when compared to wild-type and *Vsx1*-null controls.

In conclusion, my work shows that *Vsx1 P254R* is not pathogenic for corneal dystrophies in a mouse model. However, my *in vitro* studies show that *Vsx1* mutations have the ability to alter transcriptional activity and therefore still have the potential to be pathogenic in humans. Further investigation is needed to determine whether *VSX1* mutations found in disease populations are, in fact, causative for corneal dystrophies.

Table of Contents

List of Tables

List of Figures

Acknowledgments

The phrase “It takes a village” has never been truer than in this case. I want to start off by acknowledging the village of people that have contributed to me getting to this point. This includes friends, family, and colleagues and there are so many of you I surely would forget someone if I tried to list everyone so thank you for any part you have played in my time here in Victoria.

Thank you to Patrick Walter and Leigh Anne Swayne for their council as committee members, lending their expertise, opinions, and suggestions and of course their support throughout my degree and this process. Next, to Bob the man behind it all, who fostered my love for science and awarded me the opportunity of a life time and has been there every step of the way as a supervisor and as a vital part of my support network. Bob also leads a family that includes all past and present members of the Chow lab. Thank you to all of you incredibly talented human beings that played a very key role in my surviving the last three years.

I want to acknowledge my parents, Rob and Cindy, who have been pushing me to be the best version of myself since I can remember, thank you for your support emotionally, logically and financially. Thank you to my brother and sister in-law, Tony and Melodie, for being a huge part of my community on the island and for never failing to provide comic relief and to my sister Becki for her unwavering support, I love all of you. To the amazing women and coaches I share the pitch with weekly thank you for being more than just a soccer team and giving me the outlet, laughs and support I needed outside of the lab and the championship this season!

Finally, thank you to the crew of graduate students, post-docs and RAs from departments all over campus who have become a part of my family during my time at UVic. You guys have been my rock through the last year especially and there will never be enough words or drinks to express my appreciation. Here is to whatever life throws at me next and to facing it with an awesome community of humans behind me.

Dedication

I dedicate this thesis to the infamous burnout. I won.

Chapter 1 Introduction

1.1 Overview

Corneal dystrophies are classified as a group of inherited diseases that result in damage to the visual system through slowly progressive, bilateral, symmetric and non-inflammatory changes to corneal structure (Weiss et al. 2015). Posterior polymorphous corneal dystrophy (PPCD) is classified as an endothelial dystrophy and results from morphological changes to the inner most endothelial layer of the cornea (Mendoza-Adam et al. 2015, Weiss et al. 2015, Le et al. 2016). In many cases, PPCD has been associated with the corneal disease keratoconus (Gasset and Zimmerman 1974, Weissman et al. 1989, Bechara et al. 1991, Blair et al. 1992, Driver et al. 1994, Cremona et al. 2009, Lam et al. 2010, Vincent et al. 2013). Keratoconus results from a bilateral, non-inflammatory thinning of the central stromal layer of the cornea which results in astigmatism (Weiss et al. 2015, Naderan et al. 2016, Valgaeren et al. 2017). While not currently classified as a corneal dystrophy due to uncertainty surrounding its inheritance pattern, 10% of keratoconus cases do have a positive family history and are inherited in an autosomal dominant or recessive manner (Edwards et al. 2001, Weiss et al. 2015, Naderan et al. 2016). The genetic basis of these two disorders has been under investigation for over a decade and remains ongoing and controversial. The broad objective of my masters thesis was to examine the molecular mechanisms that underlie PPCD and keratoconus. Specifically, my work was focused on *VSX1*, a transcription factor-encoding gene that is associated with these diseases.

1.2 Corneal Structure, Function and Development

The most outer layer of the eye is a transparent, avascular and highly innervated tissue called the cornea. The cornea not only holds the majority of the refractive capacity for our eye but also serves as a barrier to our immediate environment (DelMonte and Kim 2015, Sridhar 2018). Maintaining corneal clarity, curvature and cellular morphology are essential for proper vision and all of these play an important role in corneal disease (Sridhar 2018).

1.2.1 Corneal Structure

The cornea consists of three cellular layers and two connective tissue layers (Figure 1). The outer most cellular layer, the epithelium, comes in direct contact with the environment and therefore must act as a strong physical barrier (DelMonte and Kim 2015). The epithelial cell layer is comprised of an outer layer four to six cells thick, of flat, packed epithelial cells that create a water tight barrier that helps prevent pathogen entry (DelMonte and Kim 2015, Eghrari et al. 2015). Below this barrier lies a suprabasal cell layer that is also two to three cells in thickness. Here basal epithelial cells are differentiating and moving anteriorly to repopulate the outer most epithelial portion. Additionally, these basal epithelial cells lay down a laminin and collagen based connective tissue layer anterior to the next cellular layer called the epithelial basement membrane (Dhouailly et al. 2014, DelMonte and Kim 2015).

Adjacent to the epithelial basement membrane lies the first acellular connective tissue layer called the Bowmans layer. Comprised of collagen fibrils, the Bowmans layer merges into the posterior stromal cell layer which is responsible for the better part of the structural integrity of the cornea (Jacobsen et al. 1984, DelMonte and Kim 2015). The stroma is the thickest of the corneal cell layers and contributes up to 85% of corneal structure (Sridhar 2018). Keratocytes populate the stroma and are interspersed with collagen, water, salts, proteoglycans and glycoproteins, much of which they are responsible for producing (DelMonte and Kim 2015, Eghrari et al. 2015).

The stroma has multiple functions including maintaining clarity through the presence of proteoglycans such as lumican. Furthermore, these proteoglycans contribute to the immune function of the cornea by regulating neutrophil migration against bacterial infections (Eghrari et al. 2015). In addition to these functions, the stromal layer holds a unique characteristic of being one of the most highly innervated tissues of the body (He and Bazan 2016). The ophthalamic division of the trigeminal nerve is responsible for sending the sensory neurons from its nasociliary branch into the stroma, with these neurons eventually innervating and terminating in the epithelial layer (DelMonte and Kim 2015, He and Bazan 2016).

Posterior to the stroma is the cornea’s second connective tissue layer, the Descemet membrane. Much like the Bowman’s layer, the structural network of the

Descemet membrane is composed mostly of collagen, though laminin, fibronectin and proteoglycans are also present (Eghrari et al. 2015). The most inner portion of this layer is laid down by the most posterior cellular layer, the endothelium. The endothelium is a single cellular layer thick. This layer has relatively low hydration however is characterized by the presence of tight junctions that help mediate movement of ions (Joyce 2003, DelMonte and Kim 2015, Eghrari et al. 2015), and gap junctions are present suggesting that endothelial cells are electrical coupled (Eghrari et al. 2015).

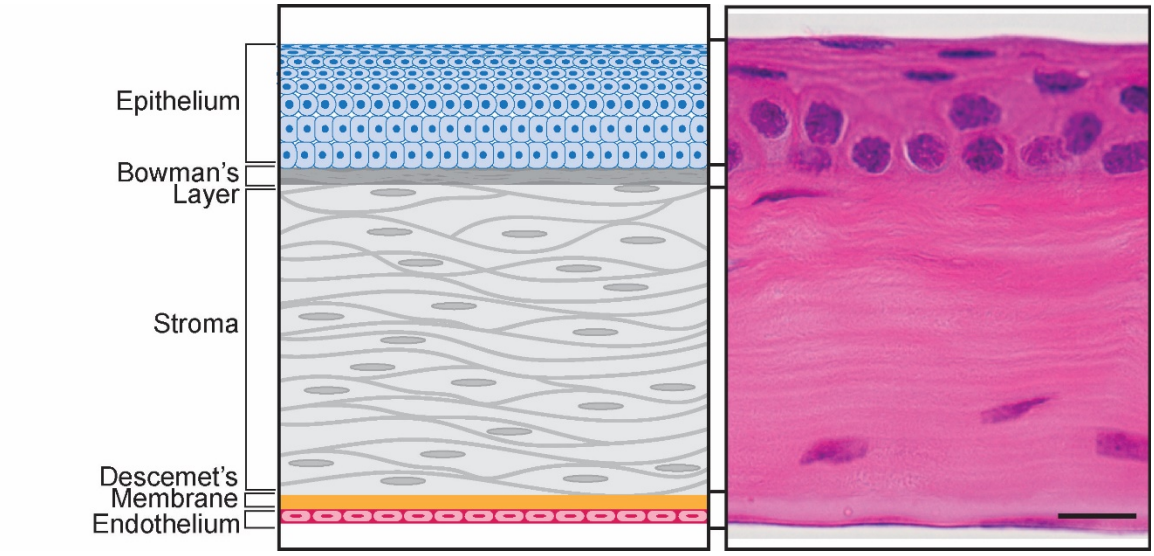

Figure 1. Schematic of the morphological layers of the most outer transparent layer of the eye called the cornea

(A) Schematic of the five morphological layers of the cornea including the three cellular layers (the epithelium, the stroma and the endothelium) and the two connective tissue layers (the Bowman's layer and the Descemet's membrane). (B) Haematoxylin stained paraffin section of the central mouse cornea showing the three cellular layers distinguished by the three different nuclear layers (A. Litke, current study).

1.2.2 Corneal Function

The outer most epithelial cell layer of the cornea serves two important functions by acting as a refractive tissue to light entering the eye and acting as a barrier between the external environment and the eye. The epithelial layer holds the majority of the refractive

capacity for the human eye due to the air tissue interface created (DelMonte and Kim 2015). Second the epithelial layer acts as a protective barrier by maintaining proper dehydration of the cornea and aiding in immune function by preventing the entry of pathogens into the inner layers of the cornea (Eghrari et al. 2015). The basement membrane of the epithelial layer also has been implicated in multiple functions including mediating the differentiation and eventual apoptosis of epithelial cells as they migrate anteriorly to populate the outer cornea (Eghrari et al. 2015).

The function of the Bowman's layer is unknown and previous studies have shown that when removed, vision remains intact (Eghrari et al. 2015). However, due to the location of the cornea's neuronal network, the Bowman's layer may play a role in sensory neuron protection (Eghrari et al. 2015, He and Bazan 2016).

The stroma contributes predominantly to the structural framework and transparency of the cornea. Due to the structural composition of the cornea, specifically the organization of collagen fibrils in the stroma, the cornea must be able to compensate for the scattering of light (Eghrari et al. 2015). The stroma overcomes this issue with multiple strategies. Changes to light refraction can be altered through the composition of proteoglycans in the stroma. Proteoglycans are able to create a more optimal distance between each of the collagen fibrils, reducing the chances light will scatter (Eghrari et al. 2015). The cornea also contains a set of water-soluble proteins called corneal crystallins that not only aid in maintaining clarity but also lower the amount of light that is scattered while passing through the stroma (Torricelli and Wilson 2014, DelMonte and Kim 2015, Eghrari et al. 2015). Additionally, the stroma contains many factors that maintain its most important characteristic of being transparent. Antiangiogenic and growth factors both aid in corneal clarity by ensuring the tissue remains avascular and that proper differentiation of keratocytes occurs (Ambati et al. 2006, Torricelli and Wilson 2014). Furthermore, the stromal layer contributes to the immune function of the epithelium and has dendritic cells and macrophages in its structural framework (Eghrari et al. 2015).

Proper dehydration of the stroma and endothelium is pivotal for maintaining corneal structure and function. The Descemet membrane plays an important role in the maintenance of dehydration as previous studies have shown breakdown and damage of the membrane can lead to severe corneal edema (Eghrari et al. 2015). The endothelium

also heavily contributes to the dehydrated state of the stroma and achieves this through tight junctions and ion channels. Specifically, a membrane localized Na^+/K^+ ATPase and the carbonic anhydrase pathway which is intracellular in its localization, are the two main contributors to maintaining hydration (Sridhar 2018). Similarly to the Descemet membrane when damage occurs to the endothelium influx of fluid in the cornea increases drastically causing edema (Eghrari et al. 2015).

1.2.3 Corneal Development

The development of the cornea and its three cellular layers occurs from the cranial ectoderm, however each cellular layer is derived from different sources of ectoderm (Lwigale 2015). Therefore, multiple processes and interactions between these ectodermal tissues must occur for their proper formation and organization.

Development of the cornea begins with the formation of an undifferentiated but organized presumptive cornea located anteriorly next to the ectoderm placode of the future lens. Here, the optic vesicles and cranial ectoderm communicate and interact bilaterally to form the early corneal epithelium (Eghrari et al. 2015, Lwigale 2015). Recent studies have started to untangle the network of factors responsible for epithelium formation and have shown that BMP signaling, that was once thought to be required for formation, is not involved (Collomb et al. 2013, Dhouailly et al. 2014). Additionally, Pax6 has been implicated in formation as differentiation of the presumptive epithelium occurs due to Pax6 being upregulated as the formation of the stroma begins (Collomb et al. 2013, Dhouailly et al. 2014).

In contrast to the corneal epithelium, the stroma and endothelium originate from the neural crest cells originating from the dorsal neural tube (Lwigale 2015). In humans the endothelium forms prior to the stroma, whereas in mice the migration of neural crest cells occurs in one wave and leads to the differentiation of both the stroma and endothelium (Lwigale 2015). Upon migration between the future epithelium and the lens vesicle, neural crest cells undergo a mesenchymal transition to epithelial cells and eventually differentiate into a single endothelial cell layer (Lwigale 2015). In humans, a second migration of neural crest cells occurs to form the stroma, the last cellular layer to form (Lwigale 2015). Once these cells have migrated between the presumptive epithelium and endothelium they begin to proliferate and produce the extracellular matrix

components that are characteristic of the stromal layer (Lwigale 2015). The components of the extracellular matrix form interactions that trap the presumptive cells as they differentiate into keratocytes (Lwigale 2015).

1.3 Corneal Dystrophies

Corneal dystrophies are classified as a group of inherited diseases that result in damage to the visual system through slowly progressive, bilateral, symmetric and non-inflammatory changes to cornea structure (Héon et al. 2002, Weiss et al. 2015). The classification system distinguishing between dystrophy and disease has evolved over the last 5 years. Debate surrounds the classical definition of dystrophy and whether not only bilaterally inherited disorders but also uni-lateral, degenerative and diseases that are heritable at a lower percentage should be included under the umbrella definition of dystrophy (Weiss et al. 2015).

Currently, for a corneal disorder to be considered a dystrophy it must have a clear pattern of inheritance. Corneal dystrophies are separated into four categories on the basis of their genetics. The first three categories include dystrophies that are well-defined in their clinical presentations. Category 1 dystrophies are classified by having a distinct gene located, mapped, identified and characterized for mutations associated with the specific dystrophy. Category 2 dystrophies lack an identified gene but have had their linkage mapped to loci in the genome. This differs come Category 3 disorders where even though well characterized in terms of how the disease presents, any genetic linkage information remains unknown (Weiss et al. 2015). The fourth and final category for classifying corneal dystrophies is reserved for disease that are not well-defined. These diseases maybe new, their clinical presentations not well understood or they may not yet be considered a distinct dystrophy on their own (Weiss et al. 2015). The investigation of corneal dystrophies remains ongoing with the goal of having all dystrophies under the umbrella of Category 1. Two diseases that have had their classification under debate for the last decade are a Category 2 dystrophy called Posterior Polymorphous Corneal Dystrophy and a disease whose status as a dystrophy remains under debate called Keratoconus (Weiss et al. 2015).

1.3.1 Posterior Polymorphous Corneal Dystrophy

Posterior polymorphous corneal dystrophy (PPCD) is classified as an endothelial dystrophy and has three distinct forms, two of which are considered Category 1 dystrophies with the third being a Category 2 dystrophy (Eghrari et al. 2015). All three forms of PPCD show an autosomal dominant form of inheritance and all three have had their loci mapped to the genome. PPCD 2 and 3 have been linked to mutations in the type VIII alpha 2 collagen (COL8A2) gene and the zinc finger E box-binding homeobox 1 gene (ZEB1) respectively (Eghrari et al. 2015). The specific genetic link for PPCD1 remains unknown but has been mapped to the genomic location of 20p11.2-q11.2 containing *VSX1* (Héon et al. 1995, 2002). Since the initial interval was identified for PPCD the linked area has been narrowed down to a 1.8 Mb region that contains 32 genes (Le et al. 2016). Studies have also aimed to determine other genes of interest that could be located in this region with *OVOL2* emerging as a strong candidate (Chung et al. 2017). However, PPCD is genetically heterogeneous and multiple genes could be responsible for disease pathogenesis (Hosseini et al. 2008).

PPCD1 (PPCD1; OMIM 122000) is an endothelial dystrophy which results from changes to the innermost single cellular layer of the cornea (Mendoza-Adam et al. 2015, Weiss et al. 2015). Morphological changes occur in the endothelial cells to become epithelial cell-like in their characteristics. This morphological shift results in sections of the endothelium to become multicellular in layering (Weiss et al. 2015, Le et al. 2016). Clinical signs of the disease are visible opacities or vesicular lesions seen in the Descemet membrane or endothelium. However, there is a high level of variability in the severity of the disease ranging from slowly progressive with many living their entire lives asymptomatic, to more aggressive forms where vision can be effected, corneal edema may occur and corneal transplantation may be required (Weiss et al. 2015). In 1974, the first case was documented where a patient with PPCD also presented with corneal symptoms of another disease called keratoconus (Gasset and Zimmerman 1974). Since then, multiple studies have reported an association between these diseases with symptoms of both diseases presenting in the same patient. This association may indicate a genetic link between the two diseases and may point to a single gene responsible for both disease

forms (Gasset and Zimmerman 1974, Weissman et al. 1989, Bechara et al. 1991, Blair et al. 1992, Driver et al. 1994, Cremona et al. 2009, Lam et al. 2010, Vincent et al. 2013)..

1.3.2 Keratoconus

Keratoconus (KTCN; OMIM 148300) is not currently classified as a corneal dystrophy due to uncertainty surrounding its inheritance patterns and the possible contribution of environmental factors to disease progression (Weiss et al. 2015, Valgaeren et al. 2017). This disease generally presents sporadically and has approximately a 1/2000 incidence in the global population. Interestingly, 10% of cases do have a positive family history (Edwards et al. 2001, Aldave et al. 2006, Weiss et al. 2015, Valgaeren et al. 2017). Keratoconus results from a bilateral, non-inflammatory thinning of the central stromal layer of the cornea (Chang and Chodosh 2013). The disease is progressive and over time the cornea becomes progressively thinner and conical in shape eventually resulting in severe astigmatism and visual impairment (Chang and Chodosh 2013, Weiss et al. 2015). Symptoms start to appear around puberty and the disease stops progressing by the age of 40 at the latest. Additionally, keratoconus is the most common reason for corneal transplantation in the global population (Wang et al. 2000, Edwards et al. 2001, Aldave et al. 2006, Dash et al. 2010).

Due to the association between PPCD and keratoconus in the same patients, the same genetic loci 20p11.2-q11.2 that was identified to be linked to PPCD has also been linked to keratoconus (Chang and Chodosh 2013). In addition, multiple other genetic loci have been associated with the disease with feasible candidate genes such as SOD1, LOX, COL4A1-4 and COL5A1 being identified (Chang and Chodosh 2013). Furthermore, because only 10% of cases are correlated to a positive family history, the pattern of inheritance for keratoconus is unclear and seems to present in both dominant and recessive forms of inheritance (Weissman et al. 1989, Wang et al. 2000, Lu et al. 2013).

1.4 *VSX1*: A Candidate Gene for Posterior Polymorphous Dystrophy and Keratoconus

1.4.1 Mapping of PPCD

In 1995 Heon et al., began the investigation into the genetic link for PPCD. The search for a possible genetic loci linked to the disease began with a single family linkage

study (Héon et al. 1995). The family had 38 members in total and 21 were affected in varying levels of severity by an autosomal dominant form of PPCD (Héon et al. 1995, Krachmer 1985). Out of the 21 affected family members, seven had disease progression to the point of corneal transplantation where diagnosis of PPCD occurred. The affected members were diagnosed as young as 4 and as old as 40 with the average age of diagnosis being 25. Along with PPCD, affected members showed additional eye conditions including glaucoma and iris abnormalities (Héon et al. 1995).

Prior to this study, four candidate loci had been identified as possible locations for association with PPCD due to other disease states and upon investigation this group concluded that there was no evidence for linkage between any of the four loci and PPCD (Héon et al. 1995). After finding no genetic linkage in the first screen, a second genome-wide screen was initiated. This screen utilized 150 nucleotide markers and upon screening the family the genomic location, 20q, was identified as being associated with PPCD (Héon et al. 1995). Narrowing the screen to 16 markers at this loci, the observed LOD scores at each marker resulted in a 30cM interval being set for a possible location for a candidate gene (Héon et al. 1995). PPCD was well-defined clinically at this point in time however, though this location was identified at the time there was no known gene in this interval that was associated with corneal development or the corneal endothelium. Though no gene was known at the time, the identification of the disease interval, narrowed the search field and opened the door for investigating a possible candidate gene that could be responsible for PPCD pathogenicity. Since the original single family linkage study the disease interval has been refined multiple times and is now narrowed to a 1.8 Mb region (Le et al. 2016).

1.4.2 Finding a Candidate Gene

With the identification of 20p11-q11, the search for the genetic basis of PPCD and keratoconus began and in 2002 the first study proposing a possible candidate gene was described. Heon *et al.*, identified the gene *Visual Systems Homeobox 1* (*VSX1*). The basis for selection was made due to the chromosomal location of *VSX1* which fell within the original and narrowed, identified region of the genome and due to its known ocular expression pattern (Héon et al. 2002). The study included 265 cases divided into four groups of patients that had PPCD, keratoconus, Fuchs' corneal dystrophy and glaucoma

in varying severity. The VSX1 coding sequence of each group and 277 controls were screened for mutations (Héon et al. 2002). From the screen six unique variants were identified with three having keratoconus, one with PPCD, one that presented with both keratoconus and PPCD and a final case that showed no clinical symptoms of either disease (Héon et al. 2002).

The six variants identified were G160D, R166W, L159M, D144E, H244R and P247R which was found in the patient with no clinical PPCD or keratoconus. Upon screening of the control population only H244R was found in two out of 277 controls (Héon et al. 2002). Excluding R166W and P247R, the four other cases had a positive family history for PPCD or keratoconus. Additional phenotypic analysis was performed on some of the cases including ERG recordings and histology. ERG recordings showed abnormal b-waves in the G160D and P247R patients and the G160D patient after undergoing corneal graft showed abnormalities through histological analysis in the Descemet membrane and the endothelium (Héon et al. 2002). Additionally, corneal graft tissue was acquired for the patient harbouring the L159M mutation and histology revealed abnormalities consistent with keratoconus in Bowman's and epithelial layer (Héon et al. 2002). Interestingly, the patients carrying the G160D and P247R mutations were parents to a proband that inherited both mutant alleles of *VSX1* and required corneal grafts at 3 months of age due to the disease severity (Héon et al. 2002). By identifying mutations found in disease populations, Heon *et al*., gave the first insight into a possible pathogenic link between VSX1, PPCD and keratoconus and the investigation into this link remains ongoing.

1.4.3 Visual System Homeobox 1 (VSX1)

VSX1 was initially identified in goldfish and belongs to the family of paired-like homeodomain transcription factors (Levine et al. 1997). The genomic location of *VSX1* is 20p11.2 and its sequence, including its 5 exons, is about 6.2 kb in length (Figure 2) (Hosseini et al. 2008).

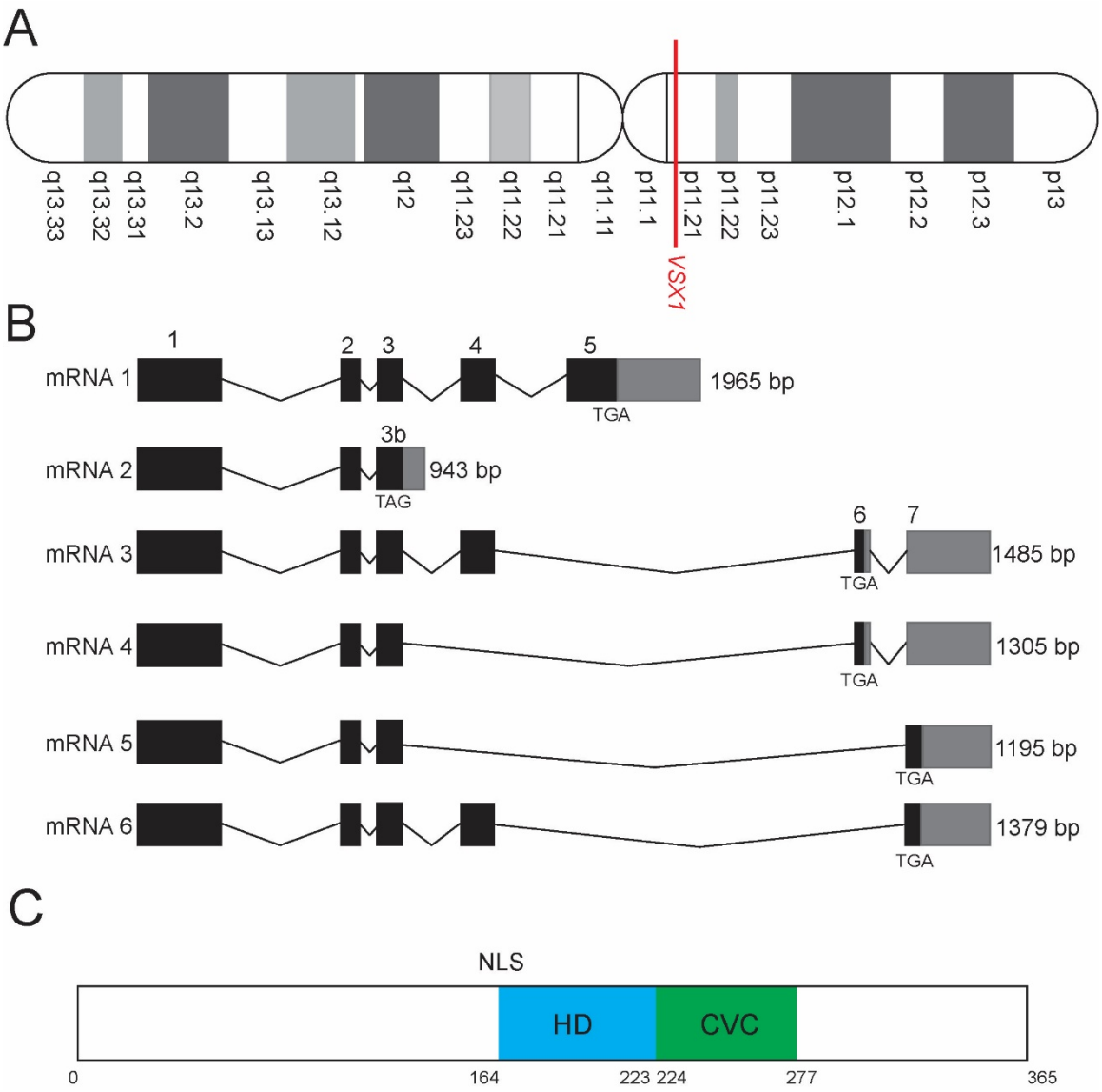

Figure 2. The paired-like homeodomain transcription factor Visual System Homeobox 1 (VSX1) a candidate gene associated with the corneal dystrophies; keratoconus and PPCD

(A) The human chromosome 20 showing the genomic location of *VSX1* at 20p11.2 which falls within the initial mapped interval of keratoconus and PPCD. (B) Adapted from (Hosseini et al. 2008) The six splice variants of *VSX1* as found in humans showing the size of each variant to the right. Black boxes indicate the seven known exons of the gene while grey boxes indicate untranslated regions. Introns indicated by the connecting black lines. (C) Protein schematic of the 365 amino acid VSX1 protein. Two high conserved domains of VSX1 are indicated in the coloured boxes; the homeodomain is designated by

the blue box while the CVC domain is indicated by the green. The nuclear localization signal (NLS) spans the region of the amino acids 162-166.

VSX transcription factors are characterized by the presence of two high conserved domains: a paired-like highly conserved homeodomain responsible for the DNA binding and an approximately 50 amino acid region known as the CVC domain named after the first three genes of this family described in mouse, fish and chick (***C****hx10,* ***V****sx1,* ***c****eh-10*). The function of the CVC domain is not fully known but has been suggested to play a role in transcriptional regulation and in ubiquitin mediated degradation (Kurtzman et al. 2000, Chow et al. 2001). Since its discovery in the adult goldfish retina, orthologues of *VSX1* have been found in many species including mouse, bovine chicken, zebrafish and *Xenopus* as well as *Drosophila* and *C. elegans* (Chow et al. 2001) .

VSX1 has been best characterized in the developing and mature retina. Its expression pattern in the mature retina is localized to the subset of bipolar cells (type 2 and 7) and can be first detected in the mouse retina as early as postnatal day 5 (Chow et al. 2001). In humans, *VSX1* expression has been reported in the neonatal cornea and embryonic craniofacial tissue. In contrast, *VSX1* has not been detected in the adult human corneal tissue (Semina et al. 2000, Héon et al. 2002, Hosseini et al. 2008). In mice, *Vsx1* expression assessed by RT-PCR, immunolabeling, and reporter gene expression has not been detected in either the developing, mature or wounded cornea (Watson and Chow 2011).

1.4.4 Requirement of VSX1 in Humans and Mice

A role for *VSX1* in the visual signaling system has been suggested in studies both in humans and in mice. Three studies have documented visual signaling defects in humans clinically associated with mutations found in *VSX1* in patients with PPCD and keratoconus using a technique called electroretinography (ERG) (Héon et al. 2002, Mintz-Hittner et al. 2004, Valleix et al. 2006). ERG is a technique that measures the electrical responses of the various types of cells in the retina in response to light stimuli. It generates two primary wave forms, the a-wave that represents the response of the photoreceptors and the b-wave which is a mixed response wave representing the other cells of the retina such as bipolar, amacrine and Müller glia cells (Weymouth and

Vingrys 2008). The first visual signaling defects associated with *VSX1* mutations were reported in the initial candidate gene study for PPCD and keratoconus by Héon et al. (2002). Here, two patients one with clinical PPCD harbouring the G160D mutation and one without clinical PPCD harbouring the P247R mutation, showed significant decreases in the ERG rod-cone b/a ratio (Héon et al. 2002). The study concluded these patients had dysfunctional retinal bipolar cells (Héon et al. 2002). Two more studies followed showing similar defects in visual signaling.

In 2004, Mintz-Hittner et al., identified visual signaling defects in a three generation family where they were able to identify two *VSX1* mutations, R131S and A256S, in four affected family members that showed abnormalities in craniofacial features, sella turcica structure and the corneal endothelium (Mintz-Hittner et al. 2004). All affected patients studied showed similar cone-mediated deficits in their ERG recordings. Two types of phototopic (i.e. bright light) flash ERG were used, a white flash on a white background and a red flash on a blue background. This allowed for the separation of the visual signaling responses for a purely cone response compared to a mixed cone/rod response (Mintz-Hittner et al. 2004). Patients showed a decrease in their 30-Hz white phototopic flash ERG or the pure cone response ERG suggesting a signaling defect in the cone bipolar cells of the retina (Mintz-Hittner et al. 2004).

The third study by Valleix et al. (2006) investigated the rod and mixed rod/cone ERG responses in a three generation family where eight members were affected with PPCD (Valleix et al. 2006). Visual signaling tests were performed on four of the family members that carried the H244R variant of *VSX1* and no significant differences or deficits were found in the scotopic responses (Valleix et al. 2006). However, upon looking at an ERG component which indicates oscillatory potentials (OPs), the first two OPs of the responses were severely decreased. Additionally, the cone b-wave of the photopic ERG responses showed a marked decrease compared to unaffected patients (Valleix et al. 2006). Valliex *et al*., concluded that patients carrying the H244R mutation have visual signaling defect that was specific to the ON bipolar cells of the retina (Valleix et al. 2006).

Similar to humans, visual signaling defects have also been observed in *Vsx1*-null mice (Chow et al. 2004). A decrease in the ERG b-wave, similar to that seen in humans,

was observed suggesting a dysfunction in cone retinal bipolar cells (Chow et al. 2004). Furthermore, ganglion cell single unit recordings revealed a dysfunction in OFF visual responses when stimulus intensity levels were above cone thresholds (Chow et al. 2004). More recently a role for *Vsx1* in the directionally selective retinal circuit which processes moving light stimuli was demonstrated (Shi et al. 2011). *Vsx1*-null retinas had prolonged excitatory input at the synapses of directionally selective ganglion cells which could possibly indicate deficits in the bipolar cells that synapse onto these ganglion cells. Together, the visual signalling defects in *Vsx1*-null mice are consistent with previous findings in humans with *VSX1* mutations suggesting that, at the level of the retina human *VSX1* mutations are pathogenic (Shi et al. 2011).

The underlying mechanism of for the visual signaling defects in *Vsx1*-null mice are due to defects in the terminal differentiation of retinal bipolar cells (Chow et al. 2004, Shi et al. 2011, 2012). Although *Vsx1*-null mice are morphologically normal in their retinal tissues (Chow et al. 2004, Ohtoshi et al. 2004) they exhibit reduced expression of OFF cone bipolar cell markers such as NetoI, NK3R, recoverin and CaBP5 (Chow et al. 2004). Interestingly, in Type 7 ON cone bipolar cells loss of *Vsx1* leads to an increase in expression of the bipolar specific genes Chx10 and CaBP5, suggesting that *Vsx1* mya function both as a transcriptional activator or repressor depending on the cellular context (Shi et al. 2011).

1.5 *VSX1* Missense Mutations Associated with PPCD and Keratoconus

1.5.1 Screening VSX1 for Mutations

Since the initial candidate gene study, around 30 studies have identified 20 missense mutations, found in both keratoconus and PPCD, disease populations that span the entirety of the *VSX1* coding region (Figure 3A, Table 1). Interestingly many of these mutations, especially those found in the two highly conserved (homeodomain and CVC) domains are highly conserved residues (Héon et al. 2002, Mintz-Hittner et al. 2004, Paliwal et al. 2009, Dash et al. 2010, De Bonis et al. 2011, Shetty et al. 2015) that are conserved in *Drosophila* and *C.elegans VSX* homologues (Figure 3B). This indicates that these mutated residues are functionally important as they are selected for over millions of years of evolution. Since the original identification of *VSX1* as a candidate gene for keratoconus and PPCD several of the variants have been identified by more than one

study group (Table 1). The extensive literature that encompasses *VSX1* mutations includes not only case-control studies but many familial studies as well. In both instances, some groups have identified *VSX1* mutations in control populations whether that be the control group in the case-control study in question or in unaffected family members (Héon et al. 2002, Mintz-Hittner et al. 2004, Aldave et al. 2005, Tang et al. 2008, Eran et al. 2009, Dash et al. 2010, De Bonis et al. 2011, Jeoung et al. 2012, Liskova et al. 2017). Across all the identified variants in *VSX1* associated with keratoconus and PPCD, the conclusions of these studies vary with some groups considering the mutations to be pathogenic, non-pathogenic and others concluding that a number of the variants may be natural polymorphisms (Conclusion: Table 1). The inability to solidify a causative link between *VSX1* and corneal dystrophies remains to this day (Liskova et al. 2017).

Ten of the *VSX1* missense mutations are localized to the two highly conserved function domains discussed earlier; the homeodomain and the CVC domain (Héon et al. 2002, Mintz-Hittner et al. 2004, Paliwal et al. 2009, Dash et al. 2010, De Bonis et al. 2011, Shetty et al. 2015). Four *VSX1* mutations (R166W, Q175H, V199L and R217H) have been identified in the DNA binding homeodomain and five (G239R, H244R, P247R, S251T, A256S and L268H) have been identified in the CVC domain. These mutations occupy positions 173, 182, 223, 246, 251, 254, 258, 263 and 275 respectively in the corresponding *Vsx1* mouse sequence (Héon et al. 2002, Mintz-Hittner et al. 2004, Paliwal et al. 2009, Dash et al. 2010, De Bonis et al. 2011, Shetty et al. 2015). The *Vsx1* mouse sequence when compared to human *VSX1* shares 71% homology. As seen in Figure 3B the majority of them occupy locations of high conservation with a couple of exceptions. V199L occupies a

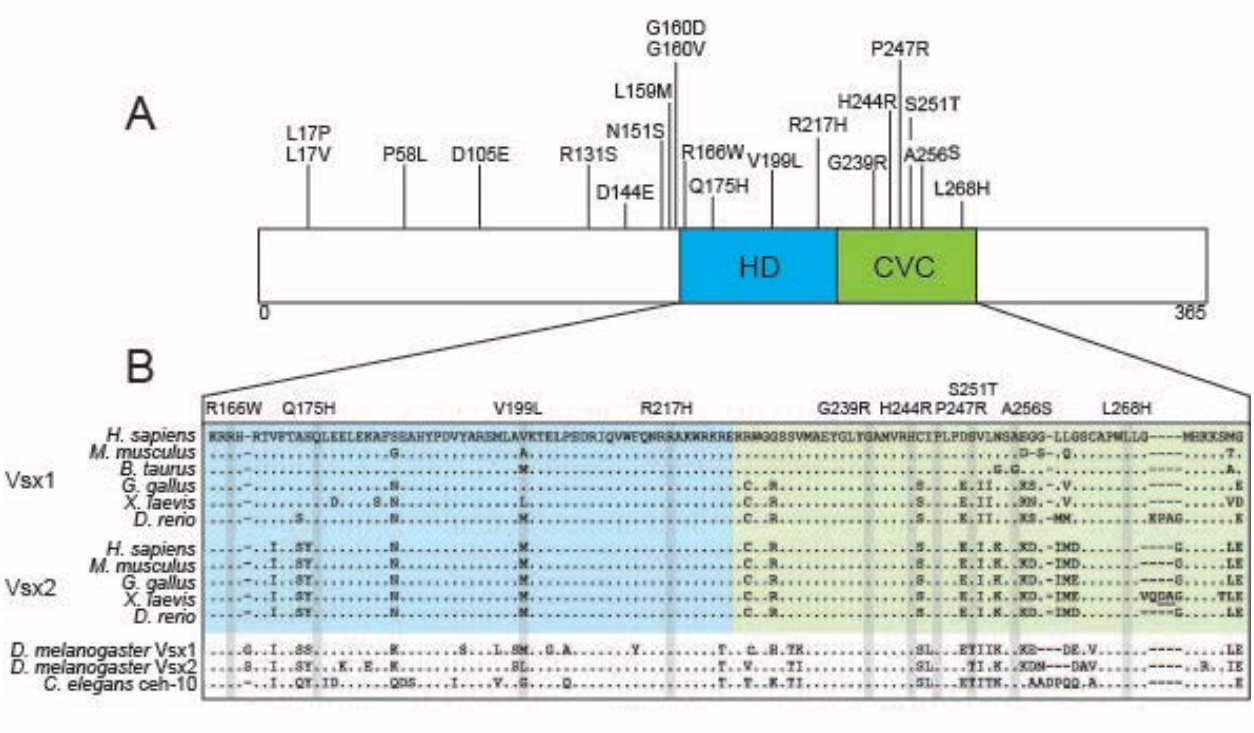

snp

Figure 3. Location and conservation of identified mutations associated with the corneal dystrophies PPD and Keratoconus in the human homeodomain protein VSX1.

(A) Schematic diagram illustrating protein position of the homeodomain (blue box) and CVC domain (green box) and distribution of human VSX1 missense mutations associated with PPD and keratoconus. (B) Amino acid alignment of the homeodomains (blue box) and CVC domains (green box) of various Vsx1, Vsx2 and other invertebrate homeodomain containing proteins. Grey boxes indicate position of 8 known human disease associated missense mutations located throughout both domains. Dots indicate conservation from the human reference sequence. Underlined *X. laevus* Vsx2 sequence indicates location of an inserted sequence (DGLQMPRRFSKPEYQQFFA). Alignments done with Clustal Omega. Sequence annotations done with Jalview.

---

residue position that shows extremely low sequence conservation across *VSX1* orthologues and similar sequence motifs (Jeoung et al. 2012). The serine residue found at position 251 in humans, though conserved throughout most vertebrate orthologues, is

changed to a threonine in invertebrate sequences. This change actually corresponds to the sequence variant, S258T, found in *VSX1* in keratoconus disease populations (Shetty et al. 2015). Due to the characteristics of the residues at these two positions I did not include them in my study. The final mutation identified in the CVC domain is L268H and was identified by Shetty e*t al* in 2015 in patients with keratoconus. The study group concluded that these change had a high probability for being pathogenic for keratoconus, however, this was identified after our mutational strategy had been completed and thus was also left out of our mutational analysis.

1.5.2 A Controversial Link

Despite the identification of *VSX1* missense mutations in disease populations many studies have discovered those identified in control groups (Table 1). Additionally, *VSX1/Vsx1* has not been detected in the adult human or mouse cornea through immunostaining, in situ hybridization, RT-PCR or reporter constructs (Watson and Chow 2011). Earlier discussion of the requirement of *Vsx1 in vivo* highlighted the effects of removing *Vsx1* entirely in the *Vsx1*-null mouse. These studies have found no overt phenotypic changes in the cornea but have revealed defects in retinal bipolar cell terminal differentiation and visual signaling defects consistent with deficits in the cone bipolar cells function retina (Chow et al. 2004, Ohtoshi et al. 2004). Together, these findings have fueled a debate around the association of *VSX1* with both PPCD and keratoconus. The ongoing search for a pathogenic link between these corneal dystrophies and *VSX1* or other genetic factors remains controversial and has even led to a published debate over this issue (Aldave 2005, Mintz-Hittner and Semina 2005).

Importantly, it was pointed out that to solidify a mutation as disease causing, requires an in-depth investigation into the protein and its function and how these mutations alter those properties (Aldave 2005). The body of research in finding the link between *VSX1* and corneal dystrophies still has these holes, as functional studies and studies in model organisms have still not been utilized. This leaves an intriguing opportunity to tackle this issue from an under-utilized angle which is what my study aims to do.

1.6 Objectives

In this study I aimed to address the controversy around the link between *VSX1* and keratoconus and PPCD by utilizing both functional protein assays and model organisms. Due to the number of variants identified in *VSX1* that are associated with the two diseases, the high conservation of the previously described residues, and the work already done on *Vsx1* in a mouse model, I hypothesize that *Vsx1* mutations in the homeodomain and the CVC will disrupt protein function and will lead to phenotypes in the visual system in a mouse model. Tackling this hypothesis involved an extensive approach using both *in vitro* and *in vivo* techniques. Here I used an *in vitro* luciferase UAS reporter system to look at changes in transcriptional activity across seven *Vsx1* mutations at highly conserved residues. Additionally, protein expresssion and subcellular localization were investigated. Two independent mouse lines harbouring one of the CVC domain mutations, P254R (variant P247R in humans), were generated using CRISPR/Cas9 gene editing. Retinal phenotypes were evaluated by measuring retina terminal marker expression and performing ERG recordings. Corneal phenotypes were examined by looking at thickness, curvature and cellular morphology. We show that five of the seven mutations trend towards an increase in transcriptional repression with a sixth change, R223H, acting as a null mutation *in vitro*. No measureable changes were seen in protein levels and subcellular localization. In *Vsx1 P254R* mice no measurable changes were seen in terminal marker expression in the retina. Furthermore, corneal phenotypic analysis showed no overt changes to cellular morphology in the stroma and endothelium of *Vsx1 P254R* mice and analysis of both corneal curvature and thickness revealed no significant differences between P254R mice when compared to wild-type and null controls. Our findings demonstrate that mutations found in disease populations can cause changes to transcriptional activity in VSX1. However, our investigation showed that the variant P254R was not pathogenic *in vivo* for keratoconus or PPCD. Our functional assays only begin to scratch the surface of how these mutations may effect VSX1 protein function and thus further research is needed to supplement these findings. A lack of phenotype *in vivo* though may be indicative of the need for a new search for a candidate gene. However, as we only investigate one *Vsx1 in vivo* variant, further studies would be

needed to rule out pathogenicity for all variants especially the R223H mutation that acts as a null mutation *in vivo*.

Table 1. Summary table of the studies that have identified mutations found in keratoconus and PPCD disease populations in the candidate gene VSX1

Variant	Disease Phenotype	Number with mutation	Total # of Affected	Familial History	In Controls	Conclusion	Source
L17P	Keratoconus	3	80	Yes	No	Pathogenic	(Bisceglia et al. 2005)
	Keratoconus	2	225/77***	1/2 Patients	No	Possible Pathogenesis	(De Bonis et al. 2011)
L17V	Keratoconus	6	53	11/53 Patients	Yes (1)	Non-pathogenic	(Jeoung et al. 2012)
P58L	PPCD	1	47	16/47 Patients	No	Pathogenic	(Vincent et al. 2013)
D105E	Keratoconus	2	85**	Yes	No	Non-pathogenic	(Liskova et al. 2017)
R131S	PPCD*	4	7	Yes	Yes	Non-pathogenic	(Mintz-Hittner et al. 2004)
	Keratoconus	1	100	Unknown	Unknown	Non-pathogenic	(Aldave et al. 2006)
	Keratoconus	2	85**	Yes	No	Non-pathogenic	(Liskova et al. 2017)
D144E	Both	1	265	Yes	Yes (Glaucoma)	Possible Pathogenesis	(Héon et al. 2002)
	PPCD	1	19	Yes	Yes (1/102)	Polymorphism	(Aldave et al. 2005)
	Keratoconus	2	80	Yes	No	Pathogenic	(Bisceglia et al. 2005)
	Keratoconus	1	100	No	Unknown	Non-pathogenic	(Aldave et al. 2006)
	Keratoconus	7	10	Yes	Yes (1/104)	Pathogenic	(Eran et al. 2008)
	Keratoconus	2*	130	Yes	No	Polymorphism	(Dash et al. 2010)
	Keratoconus	3	225/77***	No	Yes (1/200)	Possible Pathogenesis	(De Bonis et al. 2011)
	Keratoconus	3*	85**	Yes	No	Non-pathogenic	(Liskova et al. 2017)
N151S	Keratoconus	1	249	Unknown	No	Pathogenic	(Mok et al. 2008)
L159M	Keratoconus	1	265	Yes	No	Pathogenic	(Héon et al. 2002)
	Keratoconus	3	77/444***	No and Yes	Yes	Non-pathogenic	(Tang et al. 2008)
G160D	PPCD*	1	265	Yes	No	Pathogenic	(Héon et al. 2002)
	Keratoconus	2	80	Yes	No	Pathogenic	(Bisceglia et al. 2005)
	Keratoconus	1	225/77***	No	No	Possible Pathogenesis	(De Bonis et al. 2011)
	Keratoconus	2	130	No	No	Possible Pathogenesis	(Dash et al. 2010)
G160V	Keratoconus	13	249	Unknown	No	Pathogenic	(Mok et al. 2008)
	Keratoconus	6	53	11/53 Patients	Yes (3)	Non-pathogenic	(Jeoung et al. 2012)
R166W	Keratoconus	1	265	No	No	Pathogenic	(Héon et al. 2002)
	Keratoconus	2	112	Yes	No	Possible Pathogenesis	(Saee-Rad et al. 2011)

Q175H	Keratoconus	1	66	No	Unknown	Pathogenic	(Paliwal et al. 2009)
V199L	Keratoconus	6	53	11/53 Patients	Yes (1)	Non-pathogenic	(Jeoung et al. 2012)
R217H	Keratoconus	1	130	No	Yes (22/100)	Polymorphism	(Dash et al. 2010)
	Keratoconus	1	50	No	No	Non-pathogenic	(Tanwar et al. 2010)
	Keratoconus	18	85**	Yes	No	Non-pathogenic	(Liskova et al. 2017)
G239R	Keratoconus	1	225/77***	Yes	No	Possible Pathogenesis	(De Bonis et al. 2011)
H244R	Keratoconus	1	265	Yes	No	Pathogenic	(Héon et al. 2002)
	PPCD*	8	9	Yes	No	Pathogenic	(Valleix et al. 2006)
	Keratoconus	2	444	Yes	Yes (1)	Non-pathogenic	(Tang et al. 2008)
	Keratoconus	4	112	Yes	No	Possible Pathogenesis	(Saee-Rad et al. 2011)
	Keratoconus	1	47	No	No	Pathogenic	(Vincent et al. 2013)
P247R	None	1	165	No	No	Non-pathogenic	(Héon et al. 2002)
	Keratoconus	1	80	Yes	No	Pathogenic	(Bisceglia et al. 2005)
	None	1	85**	No	Yes	Non-pathogenic	(Liskova et al. 2017)
S251T	Keratoconus	3	20	Yes	No	Polymorphism	(Shetty et al. 2015)
A256S	PPCD*	4	7	Yes	No	Pathogenic	(Mintz-Hittner et al. 2004)
L268H	Keratoconus	5	20	Yes	No	Pathogenic	(Shetty et al. 2015)

R131S PPCD* & A245S PPCD* had additional visual, auditory and craniofacial deficits found

D144E Keratoconus* & P247R None* had abnormal ERGs consistent with cone bipolar cell deficits

***Indicates studies where mutations were found in unaffected family members**

****Study looked at two or more affected individuals from 85 families**

*****Indicates number of patients studied in each category of keratoconus (spontaneous/familial)**

Chapter 2 Materials and Methods

2.1 Cell lines

Human embryonic kidney (HEK) 293T cells were grown on 10 cm plates in Dulbecco's Modified Eagle Medium (DMEM) supplemented with 10% fetal bovine serum (FBS), 1% L-glutamine and 1% penicillin-streptomycin at 37ºC, 5% CO_2.

2.2 UAS Luciferase reporter assay

HEK cells were trypsinized and plated on 96 well plates at a seeding density of $0.025x10^6$ cells/well. Plates were left for 24 hours before transfection using FuGENE (Promega). Each transfection included 0.04 µg of the respective *Vsx1* or blank control construct, reporter construct and activator construct, as well as 0.005 µg of the renilla normalizing construct. Transfection master mixes were incubated for 15 minutes at room temperature before 5 µL of each master mix was added to its respective well. Plates were then incubated for 24 hours before the luciferase assay was performed. 24 hours after transfection, the assay was performed using the Dual-Glo® Luciferase Assay System (Promega) and plates were read on a Infinite 200 Pro Micro-Plate Reader (Tecan Life Sciences) according to the Dual-Glo® protocol. Firefly luminescence was normalized to renilla control luminescence. Assays were repeated to an n=5. Data was analyzed using the software GraphPad using a one way ANOVA and a multiple comparisons Dunnett's test.

2.3 Plasmids

5xGal4-4xP3-TATA-luciferase was built from an original reporter plasmid 5xGAL4-TATA-luciferase (Addgene # 46756). Four *Vsx1* specific P3 binding sites separated by 8 bp, of sequence TAATTAAATTA, were introduced downstream from five Gal4 binding sites and upstream from the TATA promoter. Original P3 sequence and 8bp separator sequence were obtained from HD4pG5EC built by J. Epstein. All plasmid modifications were confirmed with sequencing. pBXG6-HSF1 is a Gal4-HSF1 activator fusion construct containing Gal4(1-147) and residues 201-529 of the heat shock factor 1 (HSF1) kindly provided by R. Bremner (Mt. Sinai Hospital, Toronto). *Vsx1* expression

constructs were generated by Haiquan Liu (Chow Lab). R173W, Q182H, R223H, G246R, H251R, P254R and A263S were introduced into wild-type *Vsx1* by site-directed mutagenesis using the NEBaseChanger™ software to design mutagenesis primers and the Q5® Site-Directed Mutagenesis kit (New England Biolabs Inc.) to introduce mutations. For western blotting and cell immunocytochemistry, an HSV tag was cloned into pEF-*Vsx1* construct and site-directed mutagenesis was carried out in the same way for the untagged expression constructs.

Table 2. Positions of variants identified in humans selected for analysis, their corresponding sequence position in mice and the targeted sequence changes for site-directed mutagenesis

Human Variant	Mouse Variant	Sequence	
		Wild-type	Mutant
R166W	R173W	AGG	UGG
Q175H	Q182H	CAA	CAC
R217H	R223H	AGG	CAC
G239R	G246R	GGA	AGA
H244R	H251R	CAC	AGG
P247R	P254R	CCA	AGG
A256S	A263S	GCA	AGC

2.4 Western blotting

HEK cells were trypsinized and plated on 6 well dishes at a cell seed density of $0.3x10^6$ cells/well. Plates were cultured for 24 hours before transfection with the FuGENE reagent (Promega). Each transfection contained 1.0 µg of the respective *Vsx1*-HSV expression construct and 1.0 µg of a GFP transfection control construct. Transfections were incubated for 15 minutes at room temperature and cultured for 24 hours before lysate preparation. Protein determinations were done with the Pierce™ BCA Protein Assay Kit (Thermo Scientific). 15 µg of protein was separated on a 12% SDS-PAGE gel and transferred to an Immuno-Blot® PVDF membrane (BioRad). Membranes were incubated in 50% Blocking Buffer (Rockland) overnight at 4°C or for one hour at

room temperature. All washes were done with 0.1% Tween 20 TBS. Blots were incubated overnight at 4°C in a primary antibody mix containing 1:5000 goat anti-HSV (abcam) and 1:2500 mouse anti-GFP (abcam). Blots were washed and incubated for two hours at room temperature in secondary antibody containing 1:10 000 DyLight™ donkey anti-goat 800 and goat anti-mouse 680 (Rockland). Blots were imaged on Li-cor Odyssey CLx. Band intensity data was collected using the blot image software Image Studio Lite Ver 5.2. Data was analyzed using the software GraphPad using a One way ANOVA and a multiple comparisons Dunnett's test.

Table 3. Western blot antibody information

Antigen	Antiserum	Source	Working Dilution
GFP	Mouse anti-GFP	Novus (NB600-597)	1:2500
HSV	Goat anti-HSV	Abcam (ab19354)	1:5000

2.5 HEK cell immunocytochemistry

2.5.1 Cell preparation

HEK cells were trypsinized and at a seed cell density of $0.1x10^6$ cells/well were plated onto 12 well dishes containing an 18mm laminin and PDL coated coverslip (neuVitro). Plates were cultured for 24 hours before transfection. After 24 hours transfection was performed with the FuGENE reagent (Promega) with each transfection containing 0.05 µg of each respective *Vsx1*-HSV expression plasmid and 0.05 µg membrane bound GFP. Transfections were incubated for 15 minutes at room temperature and plates were left for 24 hours before fixing. After 14 hours coverslips were fixed in 4% paraformaldehyde (PFA) for 15 minutes at room temperature, washed and incubated in 1% Triton X-100 for 10 minutes. All washes were done in 1X PBS.

2.5.2 Immunocytochemistry

Coverslips were incubated in primary antibody containing 1:1000 goat anti-HSV (abcam) at 37° for one hour. Coverslips were then washed and incubated in a secondary antibody mixture containing 1:500 donkey anti-goat Alexa 555 (InVitrogen) and 1:10

000 DAPI for one hour at 37° after which they were mounted and imaged at 20X and 100X magnification on a Nikon C2 confocal microscope.

2.6 Mouse Lines

Mice were maintained on a 12 hour light/dark cycle and all experimental procedures were approved by the University of Victoria Animal Care Committee, in accordance with the Canadian Council for Animal Care (Protocol Number: 2014-023). Experimental mice were used between 6 weeks and 2 months of age or were kept housed for at least a year and a half for long term observation and analysis. Equal numbers of males and females were used for animals between the ages of 6 weeks and 2 months while long term observation mice were solely female due to housing constraints.

2.6.1 Vsx1-null Gus8.4GFP

Vsx1 ^{AltB5} (*Vsx1*-null) mice were generated by Dr. Bob Chow (Chow et al. 2004 University of Victoria, CA) on a 128SJ background. *GUS8.4GFP* mice were provided by Robert Margolskee (Roche Institute of Molecular Biology, New Jersey, New York). Mice from each strain were crossed to generate mice homozygous for *GUS8.4GFP* and either heterozygous or homozygous for *Vsx1*^{AltB5}.

2.6.2 Vsx1 P254R

Vsx1 P254R mice were generated using CRISPR/Cas9 on a C57BL/6 background at the University of Cincinnati, Children's Hospital. At amino acid position 254 a CCA to AGG mutation was introduced using the gRNA target site CTGCATTCCACTGCCGGA. In addition to the intended missense mutation, an additional silent mutation of CTG to CTT was introduced at amino acid position 255 to create a BspE1 restriction enzyme site which allows for genotyping of the P254R line. Four lines were received, 6991, 6994, 7000 and 7002, which included the P254R and silent mutation. Founder mice were crossed to wild-type C57Bl/6 mice to maintain the background and offspring were genotyped and sequenced to confirm the presence of the mutations and rule out any off target mutations that may have been introduced. From sequencing two lines 6991 and 7000, were confirmed to functional lines harbouring both the P254R mutation and the

silent genotyping mutation. Control wild-type (WT) mice were on the C57BL/6 background.

2.7 Genotyping

Genomic DNA was prepared from an ear biposy and denatured in 50 mM NaOH at 95°C for 10 minutes. Samples were then neutralized with the addition of 0.5 M Tris-HCL (pH 8.0). PCR reactions were prepared based on table 5 with the respective primer pairs listed in table 4. Reactions were run on a T3 thermocycler (Biometra, USA) with the respective annealing temperature listed in table 4. PCR products were then run by electrophoresis on a 1.2% sodium borate gel at 200V for 12 minutes and visualized using a UV Transilluminator (UVP). For the *Vsx1 P254R* mouse line an additional digestion step was required for proper visualization of PCR products. PCR samples were digested before being run on a gel with the restriction enzyme BspE1 for one hour at 37°C.

Table 4. Specific primer pairs and annealing temperatures for genotyping PCR

Mouse Line	Primers		Annealing Temperature (ºC)
Vsx1 P254R	Forward	GAGTGGTCCCTTTGTAGACCC	60
	Reverse	ATACATTGCCTCACAGTTTCAACA	
Vsx1-null (AltB5)	Forward	TTCTAGGCTGTCTAGGTCTC	55
	Reverse	TGATGGCAAAGCTTCGAAGG	
	Mutant	ATGTGGAATGTGTGCGAGGC	
Gus8.4GFP	Forward	CCGGGCCCCTCTGCTAACC	60
	Reverse	GGTGAGCTTTCCGTATGTGGC	

Table 5. Typical PCR reagent mix for genotyping of mouse strains

Reagent	Final Concentration
Forward Primer	0.5 µM
Reverse Primer	0.5 µM
10 mM dNTP	0.2 mM

10X PCR buffer + $MgCl_2$ (Gene DireX)	1X
Taq DNA polymerase (Gene DireX)	0.1 unit/µL
Ultrapure ddH_2O (Invitrogen)	-
DNA	1 µL per 20 µL

2.8 Retina immunocytochemistry

2.8.1 Tissue Preparation

Mice were anesthetized with isoflurane and euthanized by cervical dislocation. Eyes were enucleated and placed in 1X PBS (pH 7.4) and immediately had a small incision introduced into the central cornea. Eyes were then placed in 4% PFA (Electron Microscopy Science, USA, Cat. # 157-8) in 0.15M PB (phosphate buffer, PH 7.4) and fixed for 20 minutes at room temperature on a rotator. Eyes were washed in 1X PBS and cryoprotected in 15% sucrose/PB at 4°C for several hours. Followed byv30% sucrose/PB at 4°C for several hours and immediately embedded in Tissue-TEK O.C.T. (Sakura Finetek, CA, Cat. # 4583) in plastic molds and flash frozen in liquid nitrogen. Sections were cut at 16 µm thickness at -20°C using a cryostat (Leica CM1850UV; Germany) and mounted on adhesive coated slides (Newcomer Supply, USA, Cat. # 5070). The sections were air dried overnight and stored at -20°C.

2.8.2 Immunolabeling

Prior to immunolabeling slides were immersed in 1% Triton X-100/1X PBS for 30 minutes and then washed in 1X PBS. Primary antibodies were applied based on dilutions in Table 6 and incubated for either one hour at 37°C or 4°C overnight. Slides were then washed in 1X PBS before secondary antibodies were applied. Secondary antibodies conjugated to Alexa Fluor dyes (Invitrogen) were applied at 1:500 dilutions and incubated on tissue for one hour at 37°C. All primary and secondary antibodies were prepared in a solution of 1X PBS and 0.1% Triton X-100. After secondary antibody incubation slides were washed in 1X PBS and mounted with Immu-mount (Thermo Scientific, USA, Cat. # 9990402).

Table 6. Primary antibody list used for the staining of fixed and frozen retinal sections

Antigen	Antiserum	Source	Working Dilution
GFP	Goat anti-GFP	Abcam (ab6673)	1:500
GFP	Chicken anti-GFP	Abcam (ab13970)	1:500
Chx10	Sheep anti-Chx10	Exalpha Biologicals (X1180P)	1:500
PKCα	Rabbit anti-PKCα	Sigma (P4334)	1:10000
Vsx1	Rabbit anti-Vsx1	Ed Levine (Vanderbitt, TN)	1:1000
Recoverin	Rabbit anti-Recoverin	Chemicon (AB5585)	1:500
HSV	Goat anti-HSV	Abcam (ab19354)	1:1000

2.9 Confocal imaging and image analysis

Fluorescence confocal microscopy was performed using a Nikon C2 confocal microscope. Images were taken using a 20X (NA 0.75), 40X (NA 1.49) and 60x (NA 1.49) Nikon objective lens and EZ-C2 imaging software. Image quantitation was done with FiJi image analysis software and Adobe Photoshop CC 2017 was used to crop and generate single channel images when needed.

2.9.1 Quantification of Recoverin labeling

Retinas were examined for bipolar cell immunofluorescence by labeling for anti-Recoverin. Images that were used for cell counting were taken with a 20X objective from the central portion of the retina near the optic nerve. For quantitation the region of interest was the inner nuclear layer of the retina, imaging was done at the brightest level just below the point of saturation for bipolar cell somas. Images were then imported into FiJi, a threshold was set for the inner nuclear layer of the retina and retinal bipolar cell somas that were above the set threshold were counted using the cell counting plugin (Cell Counter, https://imagej.nih.gov/ij/plugins/cell-counter.html). Each experiment was repeated at least three times with at least three central retinal regions quantified. Data was

analyzed using the software GraphPad using a One-way ANOVA and a multiple comparisons Dunnett's test.

2.9.2 Quantitation of Type 7 retinal cone bipolar cell Chx10 levels

Retinas were examined for immunofluorescence by triple labeling for Chx10, GFP and PKCα. Z-stack images consisting of five optical sections were taken with the 60X objective and 4 images were taken per mouse and three mice per genotype were used. Sections with a step size of 0.45 µm were taken above and below the brightest focal plane of Chx10 intensity with the brightest Chx10 intensity obtained by setting the gain just below the point of saturation for each individual Z-stack taken. For quantitation the maximum Chx10 intensity in the Z-stack was taken for a given cell that was *Gus8.4GFP* positive and PKCα negative. *Gus8.4GFP* Chx10 levels were normalized to Chx10 levels in *Gus8.4GFP* negative, PKCα positive cells with intensity levels being quantitated in the same manner described above. Data was analyzed using the software GraphPad using a One way ANOVA and a multiple comparisons Dunnett's test.

2.10 Confocal microscopy of live corneal tissue

2.10.1 Curvature imaging

Intact eyes were enucleated, placed at the bottom of a well filled with 50% SGC5 dye (Biotium Cat # 70057) and oriented under a dissecting scope with the cornea facing up. A round 1.0mm thickness coverslip was placed over the well. Bringing the corneal apex into focus, the cornea was centered in the field of view. Images were taken using a Nikon 4X (NA 0.13) and the Nikon EZ-C2 imaging software. Corneas were imaged with the 488 nm laser and the gain was set to just above saturation for the labeled epithelial cells. Optical Z-stacks of a 4µm step were then taken from just above the brightest point of the apex down to the widest diameter, brightest location indicative of where the cornea meets the sclera. Z-stacks were taken for both the right and left eye of three mice of each genotype including adults ranging in age from 6 weeks to 2 months and long term observation adults that were at least a year and a half in age.

2.10.2 Thickness and morphology imaging

Eyes were placed in a petri dish containing 1X PBS and small incision was made at the corneal sclera border with a type 11 surgical blade (Magna). 50 µL of undiluted

SGC5 dye was injected at the point of the incision using a 30 gauge needle attached to a 1cc syringe. Eyes were then taken and placed back into the bottom of a well filled with diluted SGC5 dye and were left for a maximum of five minutes before they could be imaged. Before imaging, the dish containing the eye was flooded with 1X PBS and the eye was oriented with the corneal apex facing up under a dissecting scope. Eyes were imaged with a 40x (type of) water objective. 5 representative optical z-stacks with a 2µm step size were taken across the cornea by first focusing and centering the corneal apex in the field of view. A central stack was then taken from just above the brightest point of the epithelial cell layer down to below the endothelial cell layer where no fluorescence could be observed. Four more Z-stacks, two to both the right and left of the central stack, were then collected by moving the field of view to the right most and left most points respective to the original position and adjusting the stack range to capture above and below the epithelial cell and endothelial cell layer respectively.

2.11 Quantitation of corneal thickness

2.11.1 Thickness Quantification

FiJi image analysis software was used to reconstruct optical z-stacks of each representative portion of the cornea and Adobe Photoshop CC 2017 was used to stitch together portions of the five optical z-stacks taken from the corneas of three mice of each genotype. Z-stacks were imported into FiJi and resliced at 2µm setting. The most central 50 optical sections of the central corneal stack were made into a maximum projection. Features were matched between adjacent stacks ensuring that the most central 50 optical sections were used for maximum projection in each stack. The five resulting maximum projections were then imported into Adobe Photoshop and were stitched together to make one representative image of the cornea. The resulting single image was then brought back into FiJi where lines perpendicular the corneal surface were drawn through the thickness of the cornea. Intensity plots were then used to measure the number of pixels from the brightest top layer (representative of the epithelial cell layer) and the brightest bottom layer (representative of the endothelial cell layer) and were converted into corneal thickness using the specified value of 0.62 µm/pixel used during imaging. Two measurements were made in both of the most peripheral portions of the reconstructed

cornea and the most central portion. Data was analyzed with the software GraphPad using a one way ANOVA and a multiple comparison Dunnett's test.

2.12 Corneal Histology

2.12.1 Tissue preparation and staining

Enucleated eyes were placed in 2.5% glutaraldehyde fixative for two hours at room temperature on a rotator. After fixation eyes were then washed with 70% ethanol and then dehydrated in 70% ethanol for 48 hours before embedding. Eye samples were sent to Wax-IT Histology Services (Vancouver, BC, Canada) for paraffin embedding, sectioning and staining. Eyes were oriented with the optic nerve positioned to the right and the side of the eye on the embedding surface. Cross sections of 4µm thickness were taken from the central portion of the cornea starting at the optic nerve as a landmark. Sections were then stained with hematoxylin and eosin and mounted.

2.12.2 Imaging and analysis

Stained corneas were imaged in bright field using Nikon Digital Sight DS-U1 camera and the Nikon ACT-2U control software. Images were either taken with a Nikon Plan Apo 20x (NA 0.75) or a Nikon Apo TIRF 60x oil (NA 1.49) objective. For analysis of corneal morphology five images were taken to capture the entirety of the cornea with the 20x objective. Adobe Photoshop CC 2017 was used to visualize endothelial cell morphology. Four stained sections for each mouse and three mice from each genotype were observed.

Chapter 3 Results

3.1 *Vsx1* transcriptional activity and protein levels

A previous study has shown that wild-type *VSX1* can function as a transcriptional repressor *in vitro* (Dorval et al. 2005). This study found that when the mutation R166W (mouse R173W), a mutation found in the homeodomain and is associated with PPCD and keratoconus, is expressed in *VSX1* binding activity of the protein is reduced (Héon et al. 2002) and the mutation impairs *VSX1* function causing a reduction in transcriptional repression *in vitro* (Dorval et al. 2005). Aside from this, a more thorough investigation of how mutations affect VSX1 function has not been done. To address this, I designed a luciferase transcriptional activity assay based this previous study (Dorval et al. 2005).

I examined seven different mutations in mouse *Vsx1* expression constructs to determine if there were changes in transcriptional activity *in vitro*. These mutations were selected based on their location in two highly conserved domains of *VSX1* as well as the high conservation that occurs at each individual residue consistent down to *Drosophila* and *C. elegans.* The reporter construct had two key areas upstream including five upstream activator sites (UAS) that are specific for Gal4 binding and four P3 homeodomain binding sites (Figure 4A). A fusion activator protein was co-transfected allowing Vsx1 repressor activity to be measured. Cells were transfected with the described reporter activator and the respective Vsx1 expression constructs and utilizing a luciferase assay, changes in transcriptional activity were measured relative to a normalizing renilla construct also included in transfection. As previously shown, wild-type Vsx1 acts as a transcriptional repressor in vitro (Figure 4B). Interestingly, R166W or indicated as the R173W mutation for the amino acid position found in mice, did not lead to a loss of repressor activity as in the previous study discussed (Dorval et al. 2005). Five of the seven introduced mutations trended towards being gain of function mutations in that they showed an increase in transcriptional repression. In contrast mutation, R223H, showed a significant difference in the activity of Vsx1 in vitro and acted as a null mutation removing all repressive function similar to the “No Vsx1” control.

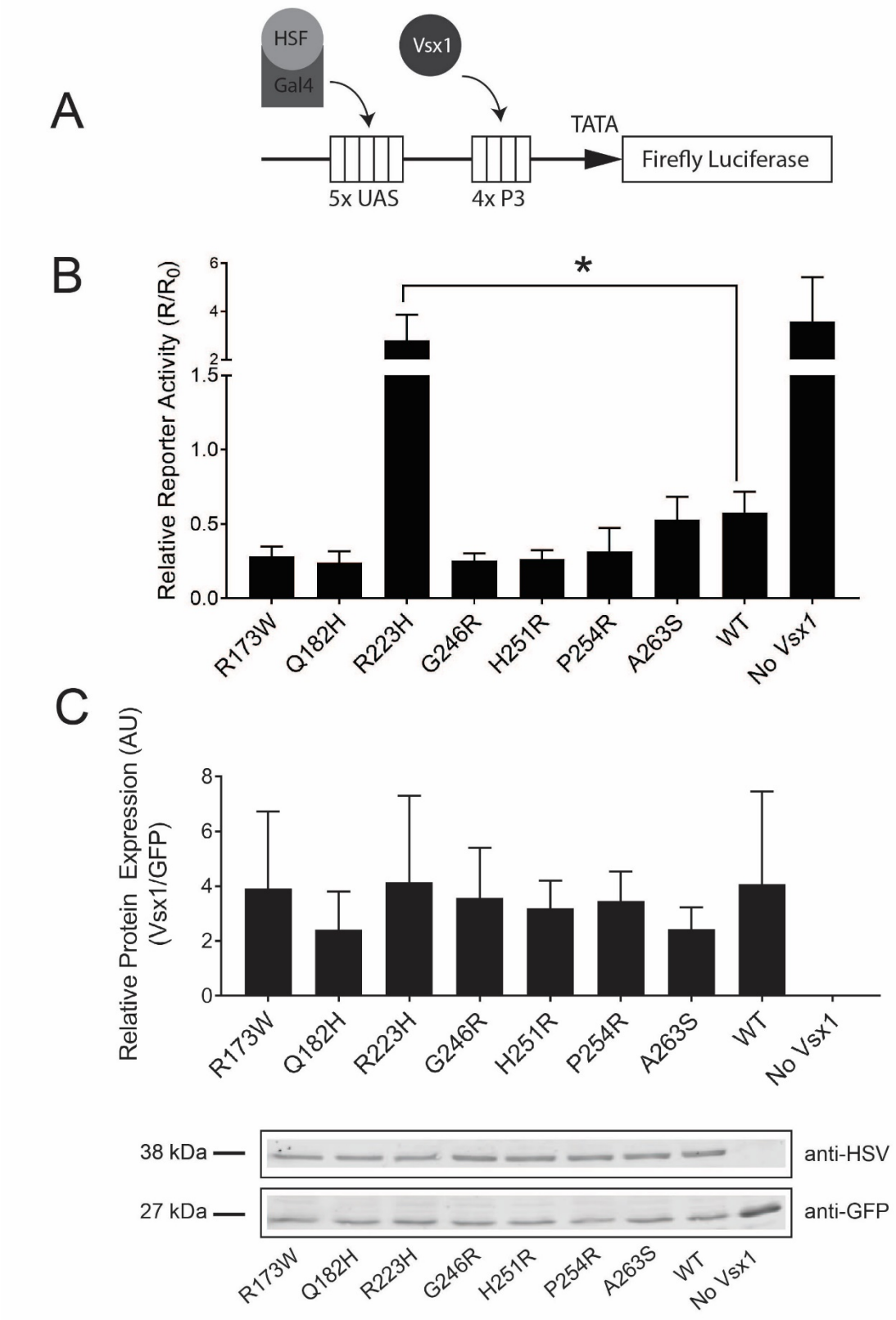
A
HSF
Gal4
Vsx1
TATA
Firefly Luciferase
5x UAS
4x P3
B
Relative Reporter Activity (R/R0)
*
R173W
Q182H
R223H
G246R
H251R
P254R
A263S
WT
No Vsx1
C
Relative Protein Expression (AU)
(Vsx1/GFP)
38 kDa
27 kDa
anti-HSV
anti-GFP

Figure 4. Effects on transcriptional activity and protein levels of in vitro when mutations found in disease populations are introduced into Vsx1

(A) Schematic of the 5xGal4-4xP3-TATA-Luciferase reporter construct designed for the transcriptional activity luciferase assay. P3 (TAATTAAATTA) sites were introduced upstream of the TATA promoter element of the original reporter construct already containing the five UAS elements. HSF-Gal4 activator fusion and Vsx1 binding locations indicated. (B) Relative reporter expression, normalized to a renilla control construct, in vitro. Cells were transfected with reporter, Vsx1 expression, activator and control constructs and a luciferase assay was applied to determine activity levels. Vsx1 expression constructs had one of the seven mutations displayed on the bottom of the graph introduced. A One-way ANOVA and a Dunnett's multiple comparisons test were performed (n=5). R223H mutation was revealed to a p-value equal to 0.0002 (C). anti-HSV western blotting of transfected HEK lysates of mutated and wild-type Vsx1 expression constructs. Vsx1 transfection efficiency was normalized to a co-transfected GFP control construct. No significant differences were found through a One-way ANOVA.

Next we wanted to determine whether changes in Vsx1 in transcriptional activity might be due to changes in Vsx1 protein levels. Protein expression, of mutated mouse Vsx1 expression constructs, were analyzed via western blot analysis and quantification indicated no changes in protein expression when Vsx1 mutations were present when compared to wild-type Vsx1 and normalized to a GFP transfection control (Figure 4C). This suggests that protein expression is not altered by the mutations in *Vsx1* and therefore is not responsible for the observed changes in transcriptional activity.

3.2 Investigating subcellular localization changes to Vsx1 *in vitro*

Wild-type VSX1 is normally localized to the nucleus (Kurtzman and Schechter 2001, Knauer et al. 2005) and previous studies have shown that disruption of the VSX1 sequence especially at the location of the nuclear localization signal (NLS) (amino acids 162 – 166) can result in mislocalized protein to the cytosol of cells (Knauer et al. 2005). Therefore, I wanted to determine whether mutations located in the homeodomain and CVC domain of *Vsx1*, affect subcellular distribution especially for mutations occurring in

or immediately downstream of the NLS. To study this we transfected HEK cells with wild-type or mutated *Vsx1* and co-transfected cells with a membrane localized GFP to observe ultrastructure of the cells. Additionally we stained with a nuclear stain to determine whether VSX1 expression co-localized to the nucleus. Cells co-transfected with VSX1 and GFP showed no changes to sub-cellular localization (Figure 5A-H). This suggests that mutations in VSX1, even those located directly in or immediately downstream to the NLS, do not alter subcellular localization of the protein and therefore mislocalization does not play a part in the observed changes in transcriptional activity *in vitro*.

Figure 5. No changes to subcellular localization of Vsx1 harbouring mutations associated with PPCD and keratoconus when compared to nuclear localized wild-type Vsx1.

(A-H) HEK subcellular localization of transfected wild-type Vsx1 and expression constructs harbouring one of seven mutations found in PPCD and keratoconus disease populations. Co-transfection with a membrane localized GFP to show overall HEK cell structure and stained with nuclear DAPI to show nucleus. Scale bar indicated in (H) represents 25 µm.

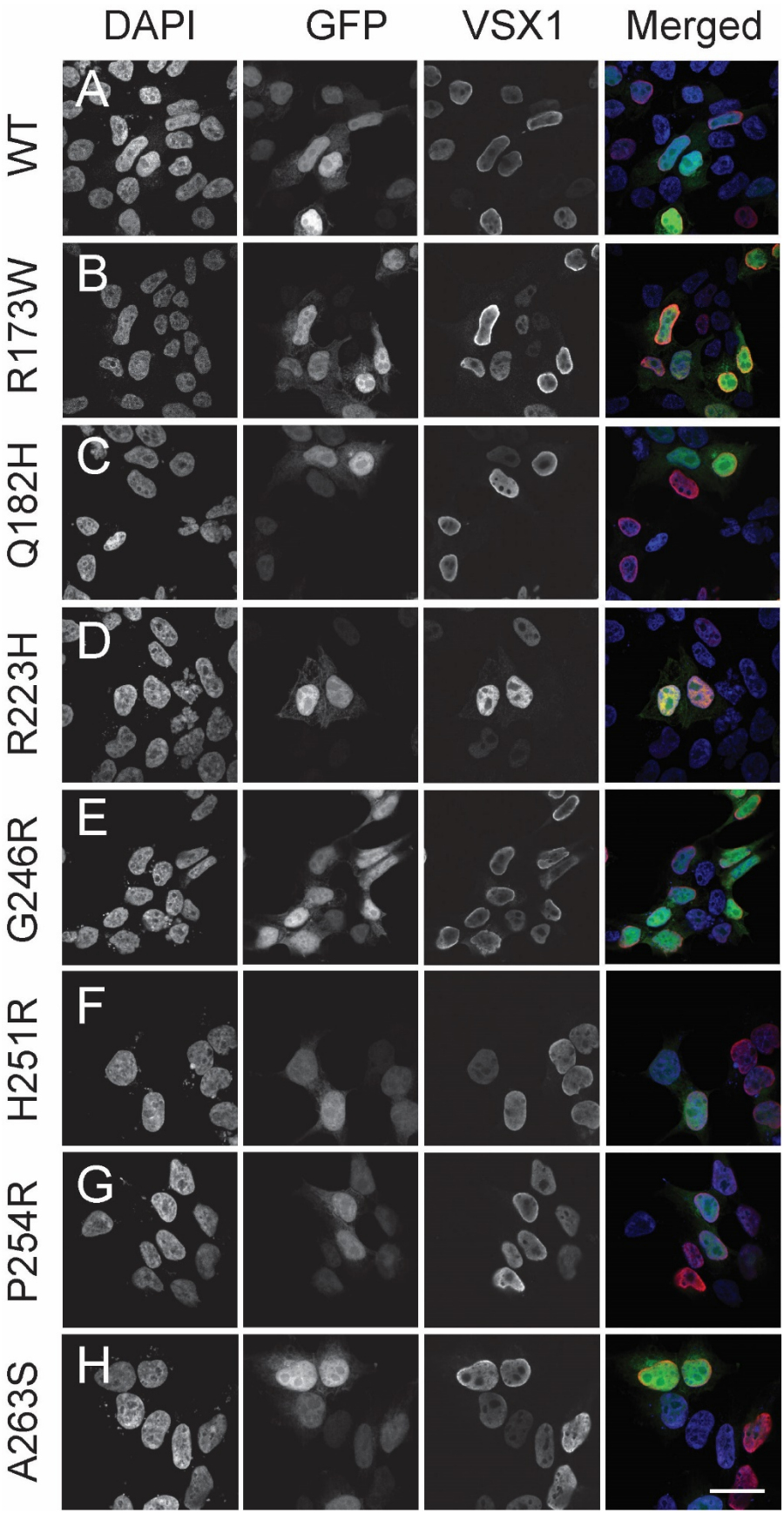
DAPI
GFP
VSX1
Merged
A
WT
B
R173W
C
Q182H
D
R223H
E
G246R
F
H251R
G
P254R
H
A263S

3.3 Generation of a mouse model to study the pathogenicity of *Vsx1* mutations

As discussed earlier, research surrounding the pathogenicity of *VSX1* mutations for PPCD and keratoconus in humans as solely focused on disease and control populations and the identification of mutations in these populations. Only a select few studies have investigated the effects of *VSX1* mutations on function (Dorval et al. 2005) and none in the field have attempted to express these mutations in another model. To address this, I introduced one of the previously described mutations in a mouse utilizing Clustered Regularly Interspaced Short Palindromic Repeats (CRISPR) Cas9 genome editing. With CRISPR-Cas9, a CVC domain mutation found at amino acid position 247 in humans or in the case of the mouse position 254 was introduced. This mutation, P254R, results in a missense change from the native proline residue to an arginine residue. This mutation was chosen based on the nature of the mutation as it is predicted to be 85% deleterious to protein function (Bendl et al. 2014) and its location in the highly conserved CVC domain in an amino acid that's conserved in *Drosophila* and *C.elegans*, and due to its identification in three separate publications.

Generation of the P254R mouse involved the introduction of two mutations into the sequence of *Vsx1* using the underlined target guide RNA (gRNA) sequence (CTGCATTCCACTGCCGGACAGC) shown in the wild-type (WT) allele (Figure 6A). Each of these mutations is shown in the knock-in (KI) allele in blue with the original sequence changes highlighted in grey. The first mutation introduces a sequence change of CCA to AGG leading to the described proline to arginine residue missense change. A second silent mutation was introduced downstream of the missense mutation and resulted in a G to T sequence change but not a change in the leucine residue located at this position. This mutation introduced a restriction site for the enzyme BspE1 and was used for the genotyping strategy of the *Vsx1 P254R* mouse line (Figure 6C). The primer pair utilized for genotyping results in a WT product of 440 bp seen as the top band in the representative gel (Figure 6D). The primer pair captures the mutation area and the restriction site as seen in Figure 6C and restriction digest of the PCR product with BspE1 results in visualization of the KI allele and the lower two bands at 233 and 207 bp (Figure 6D).

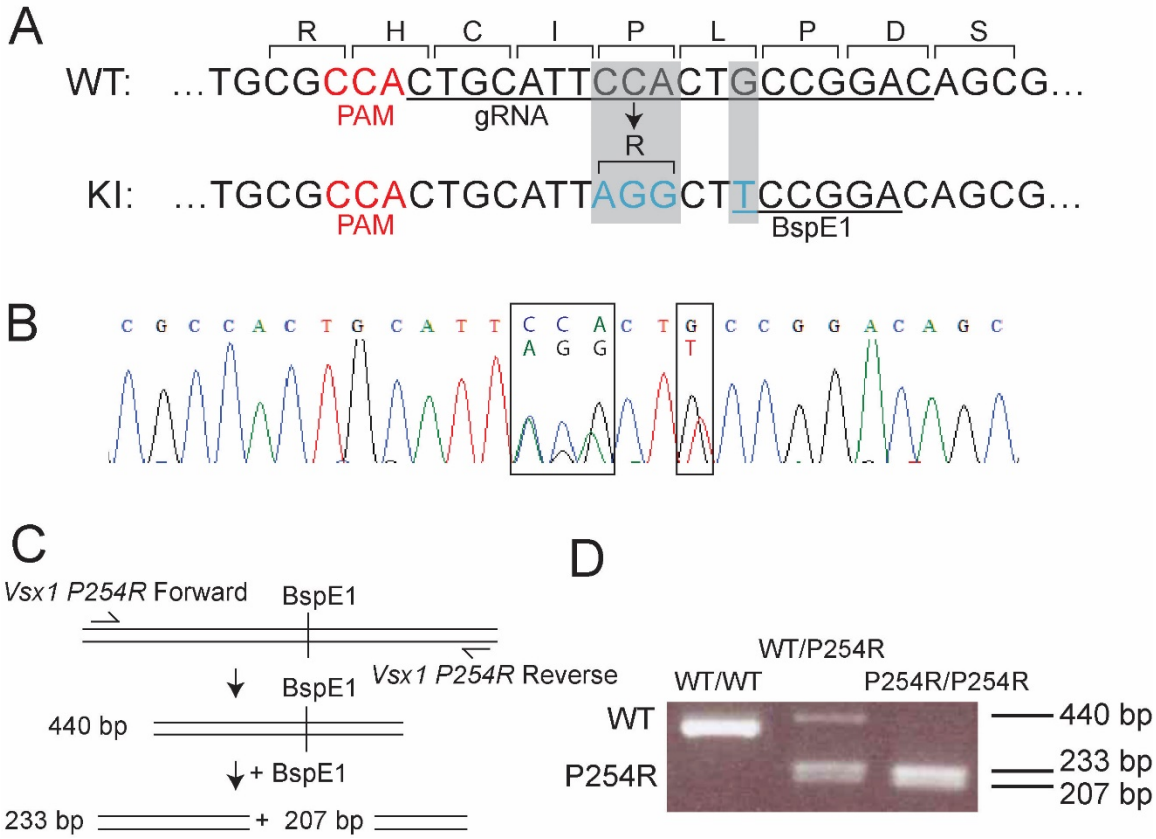

Figure 6. Investigating the pathogenicity of *VSX1* mutations for PPCD and keratoconus in a generated mouse model *Vsx1 P254R* of the P247R mutation found in the CVC domain of *VSX1*

(A) Schematic showing the strategy for the mutation of the proline residue at position 254 to a arginine using CRISPR. PAM and guide RNA (gRNA) recognition sequences indicated in red and underlined respectively. One letter amino acids codes indicated for the surround residues. Silent mutation also shown in blue that introduces a BspE1 restriction site for genotyping strategy. (B). Chromatogram showing sequence of a heterozygous mouse harbouring both the missense and silent mutations. (C). Genotyping strategy for *Vsx1 P254R* mouse line. (D) Representative gel showing the PCR and digest products of all three genotypes from the P254R mouse line with WT product at 440 bp and the mutated allele shown as two fragments due to the BspE1 restriction site.

Mice were sequenced for the mutations and three out of four potential founders were identified. From these I confirmed two independent lines harboured the desired mutations. The coding regions of *Vsx1* were sequenced to insure there were no off-target changes. Figure 6B shows an example of the sequencing chromatogram of a heterozygous mouse carrying both the sequence for the WT and KI alleles.

Mice homozygous for the *Vsx1 P254R* mutation were chosen for analysis and heterozygotes were not used in our analysis. Homozygotes were selected on the reasoning that if the mutation was pathogenic homozygotes would have a more serious phenotype. Additionally, in the *Vsx1*-null mouse significant phenotypic changes were only visible in homozygous mice when compared to wild-type controls (Chow et al. 2004).

Furthermore, mice of various age groups were used for analysis based on the progressive nature of these diseases. In both Keratoconus and PPCD symptoms of the disease can be detected between the ages of 20 and 40 with disease progression occurring into later adulthood. I chose adult mice from two different age ranges, the first between 6 to 10 weeks of age and the second group containing mice that were at least a year and a half in age or older. 6 to 10 week old mice were chosen due to the already characterized phenotypes of *Vsx1*-null mice that present in adult mice of 6 weeks old and are stable throughout adult life. The long-term mice were chosen to insure that phenotypes occuring later in life, as they do in humans, were not missed.

3.4 Morphological analysis of the cells, thickness and curvature of the *Vsx1 P254R* mouse cornea

PPCD as previously described is an endothelial corneal dystrophy resulting from epithelial cell-like morphological changes to the inner single endothelial cell layer (Weiss et al. 2015, Chaurasia et al. 2017). These morphological changes to the endothelial layer have been found in patients with PPCD harbouring mutations in *VSX1*, however, as previously discussed the pathogenicity of *VSX1* mutations for PPCD and keratoconus remains controversial.

3.4.1 Investigating cellular morphology of the corneal epithelium, stroma and endothelium using whole eye histology

To address whether the *Vsx1 P254R* mutation in mice led to a phenotype I examined histological sections from paraffin embedded mouse corneas from adult mice between 6 weeks and 2 months old or from mice kept for long term observation that were a year of older in age. These sections were then stained with hematoxylin and eosin (H&E) and the endothelial cell layer was imaged for the entire cornea of four representative sections of the central cornea (Figure 7). When compared to wild-type neither *Vsx1 P254R* or *Vsx1*-null corneas of adult mice up to two months in age or *Vsx1 P254R* corneas of mice of at least a year did not show any morphological cell changes in the endothelial cell layer characteristic of the abnormalities associated with PPCD. Additionally, histology reveal that across all genotypes, all three cellular layers of the cornea appear normal and showed no overt phenotypic changes compared to wild-type mice.

3.4.2 Utilizing ex vivo confocal microscopy to analyze corneal characteristics

Few studies have examined corneal thickness and curvature of unfixed corneas *in vivo*. Approaches using fixed tissue examine corneal morphology and thickness, have a caveat that this fixation process can alter the corneal thickness, specifically that of the stroma (Henriksson et al. 2009). Additionally, sectioning of frozen or paraffin sections can lead to holes or damage to the cornea structure and although it may not alter cellular morphology, rarely leaves the ultrastructure of the cornea intact (Henriksson et al. 2009).

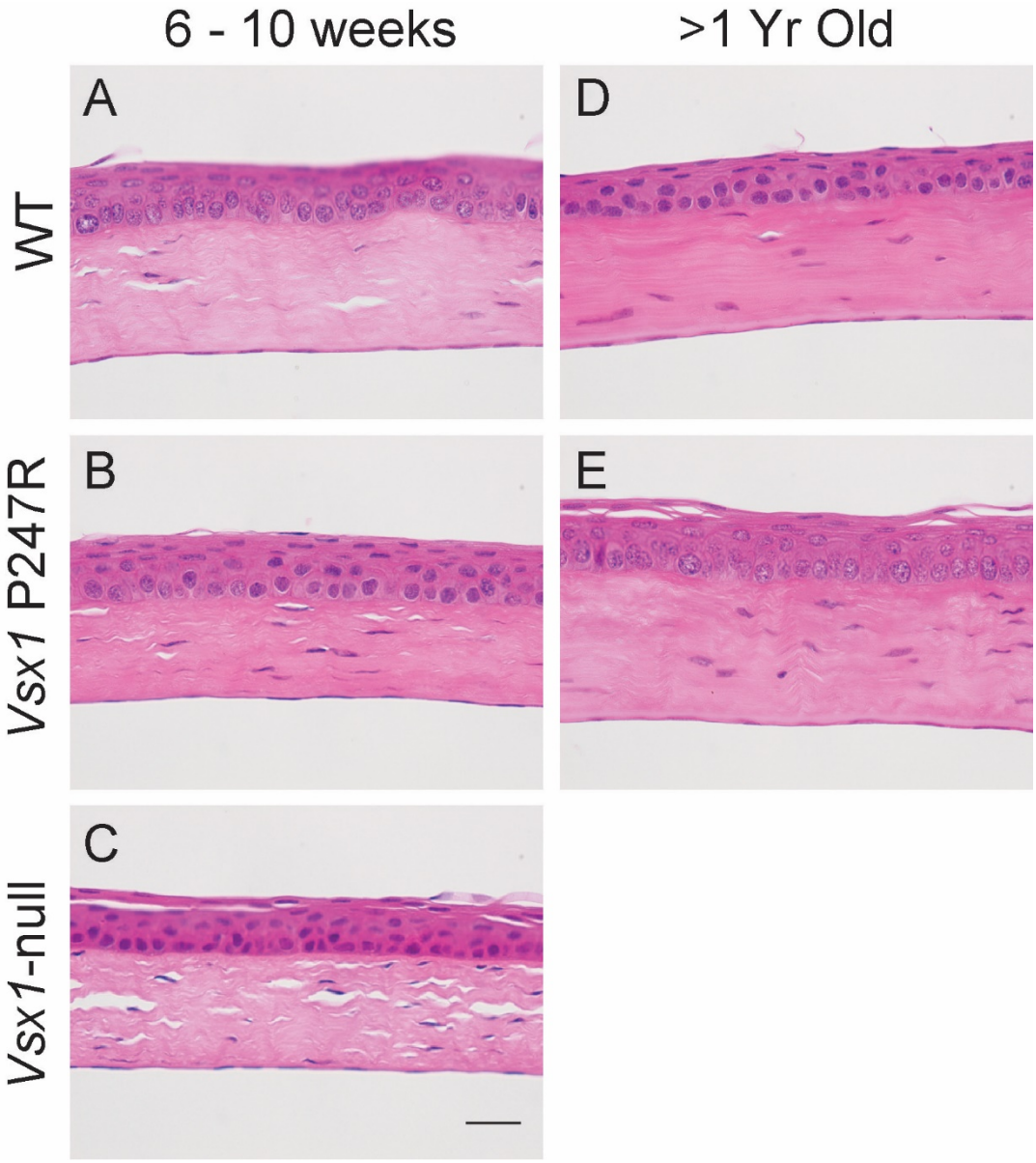

Figure 7. Histological analysis of the mouse cornea shows no morphological differences in the five layers of the cornea associated with PPCD or keratoconus. (A-C) Hematoxylin and eosin (H&E) staining of paraffin embedded adult mouse corneas ranging in age from 6 weeks to 2 months old for three genotypes; wild-type, homozygous *Vsx1 P254R* and *Vsx1*-null mice. (D-E) H&E stained cornea sections of paraffin embedded adult mouse corneas of long term mice kept for at least a year or longer before processing for both WT and homozygous *Vsx1 P254R* genotypes. Scale bar 50 µm.

3.4.2.1 Whole eye ex vivo confocal microscopy

To address the caveats to fixation and sectioning I wanted to design a method that would allow for the observation of the curvature and thickness of mouse corneal tissue *in vivo* with minimal to no impact on corneal morphology. *In vivo* confocal microscopy has been used to evaluate morphology of the layers of the cornea in a clinical setting (Mazzotta et al. 2008). Utilizing confocal imaging and a membrane bound dye SGC5 I developed a two-step protocol for imaging corneal morphology, thickness and curvature. Immediately following removal from the mouse, eyes were placed in a well of diluted dye and covered with a cover-slip. Utilizing a 4X objective that captured the entirety of the eye, confocal z-stacks were taken, beginning just above the cornea and imaged down to the limbal region where the cornea and sclera met (Figure 8A). An average intensity projection was then created to get the curvature of the most central region of the cornea. Due to the inherent properties of the epithelial cell layer of the cornea (Eghrari et al. 2015), diffusion of the dye throughout the other layers of the cornea was not observed when eyes were just placed in undiluted dye. After imaging of the corneal surface had been completed, the eye was removed and placed in solution where a small incision was made along the corneal sclera interface and a small amount of undiluted dye was introduced into the incision with a needle. We found that this approach had robust labeling of all corneal cell layers. The whole eye was then imaged using a 40X water immersion objective. Five representative stacks starting in the most central region of the cornea and moving peripherally to the right and left of the starting position (Figure 8A). Each of the five stacks was used to create maximum projections that corresponded to a 50 µm section of the central most portion of the cornea (Figure 8B). Individual images in the stacks also allowed for the observation of any overt phenotypic changes to cellular morphology in the epithelial, stromal and endothelial cell layers to supplement the histological paraffin sections.

3.4.2.3 Investigating changes to corneal thickness utilizing whole eye ex vivo confocal microscopy

Keratoconus presents as irregular astigmatism of the cornea and results from stromal thinning in the cornea (Valgaeren et al. 2017). Measurements of overall corneal thickness maybe unveil phenotypic changes due to disease states. To determine whether

Vsx1 P254R mice had any irregularities in corneal thickness we utilized our *ex* vivo confocal microscopy strategy described above and the landmarks with the upper most fluorescence representing the epithelium and the lower the endothelium (Figure 9A). These two landmarks allow for a line to be drawn perpendicular to the surface of the cornea and an intensity plot to be generated for that position in the cornea (Figure 9B). A consistent intensity threshold was set and the beginning and end of the two biggest peaks were used to determine thickness. The cornea in humans maintains a consistent thickness across its entirety. In mice, however, this is not the case as previous studies have shown the peripheral and central cornea naturally have different thicknesses. Due to caveats previously mentioned with classical fixation and sectioning techniques, there remains a debate around how thickness varies across the cornea in mice with some studies showing the peripheral cornea being thicker than the central and others with the central being the thicker portion with thinning of the cornea occurring as you move peripherally (Henriksson et al. 2009). To address this, I separated my measurements for the peripheral and central cornea. Two measurements were taken in each respective peripheral section and three measurements were taken across the central region. Three mice of each genotype were used between 6 and 10 weeks while another three mice were used for mice of age greater than one year (Figure 9C). From our method, we did see an observable difference in thickness between the peripheral and central cornea with the more peripheral sections being thicker in comparison. However, when overall peripheral and central measurements were compared across genotypes no significant differences were observed (Figure 9C).

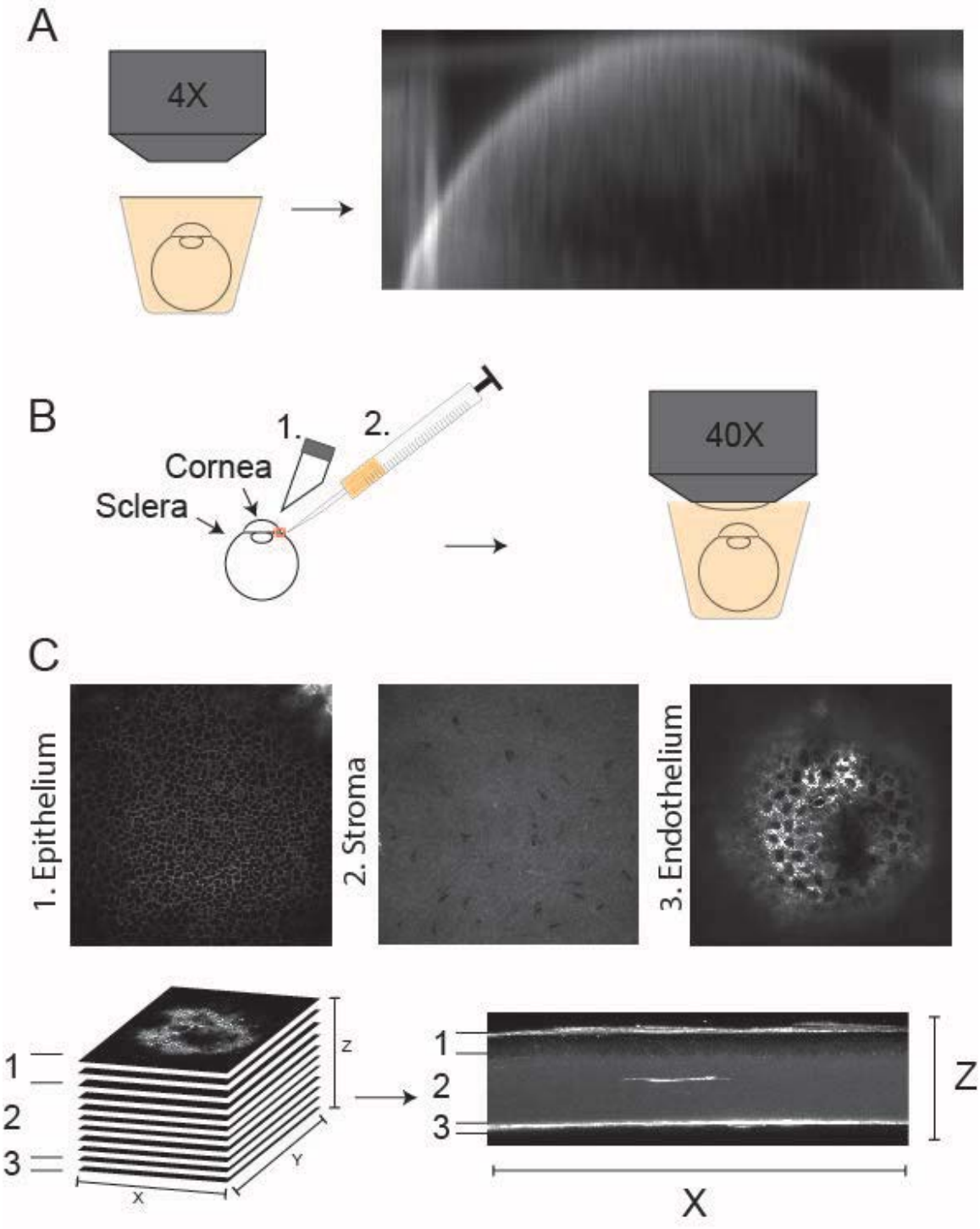

Figure 8. *Ex vivo* confocal microscopy strategy for analyzing corneal outer curvature, thickness and morphology in whole eyes of mice utilizing a membrane bound dye for visualization

(A) Schematic showing the three steps utilized to obtain corneal outer curvature and overall thickness through *ex vivo* confocal microscopy. Immediately after removal eyes are placed in diluted dye and imaged on a 4X objective to obtain a representative stack of the outer curvature. Average intensity stacks were then created for each eye to get the most central curvature of the cornea. Following imaging, a small incision in the limbal region of the eye is made with a razor and undiluted dye is introduced into the incision with a needle. Corneal thickness was then imaged through in its entirety using a 40X water objective in diluted dye. (B) Strategy for maximum reconstruction of a 50µm central region of the corneal for analyzing thickness. Z-stack images were resliced and the most central images representing a 50 µm section in the Y axis were taken for the five representative stacks taken across the whole cornea. Maximum projections were used for thickness analysis.

3.5 Phenotypic analysis of the retina in the *Vsx1 P254R* mouse and *Vsx1*-null mouse

The debate surrounding the pathogenicity of *VSX1* in cornea dystrophies in humans has sparked the search for other phenotypes *in vivo* that may be correlated to *VSX1* dysfunction. As previously discussed studies have found abnormalities in the ERG recordings of patients harbouring mutations in *VSX1* (Héon et al. 2002, Mintz-Hittner et al. 2004, Valleix et al. 2006). These abnormalities are consistent with a dysfunction in the cone bipolar cell circuitry of the inner retina. This is also consistent with the expression pattern of VSX1 in adults that is isolated to the inner nuclear layer (INL) of the retina (Chow et al. 2001). Additionally, when *Vsx1* is knocked out in mice, similar visual signaling defects seen with ERG recordings and single cell recordings consistent with abnormalities in the retina cone bipolar circuitry (Chow et al. 2004, Ohtoshi et al. 2004, Shi et al. 2011). We therefore wanted to determine whether visual signaling defects in our *Vsx1 P254R* mice.

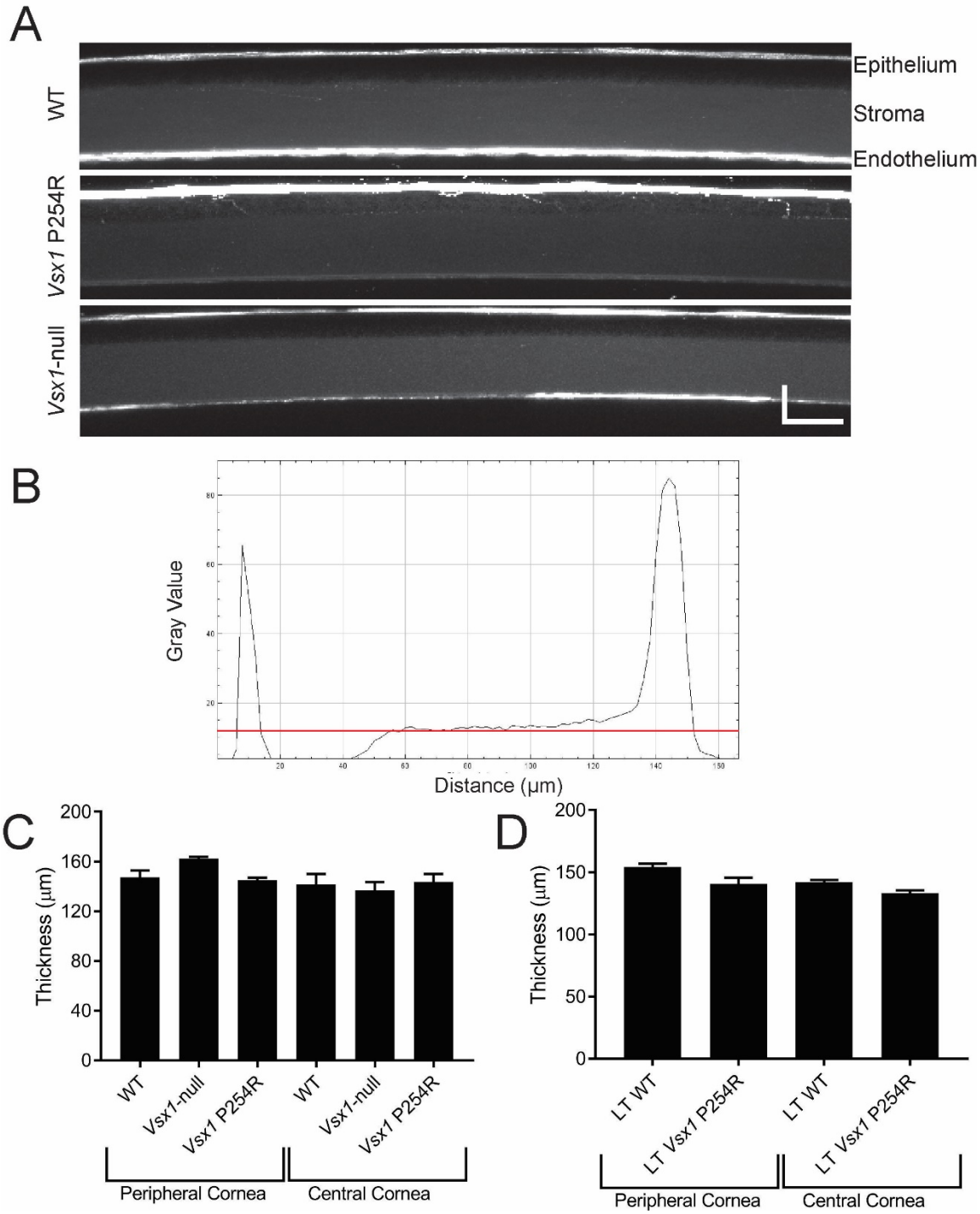

Figure 9. Analysis of corneal thickness through *ex vivo* confocal microscopy of *Vsx1 P254R* and *Vsx1*-null mice

(A) 50 µm maximum projections of the most central stack taken through the central apex of the cornea of wild-type, *Vsx1* P254R and *Vsx1*-null mice that were injected with SGC5

dye. All three cellular layers are visible in the first panel with the upper most fluorescence representing the epithelium, followed by the large stromal layer and finally the lower fluorescence representing the endothelium. Scale bar equal to 50 µm (Y) by 25 µm (X) (B) Representative intensity plot of a line drawn through the thickness of the cornea, perpendicular to the surface, on a maximum projection. Red line indicates the intensity threshold value chosen to acquire measurement values. (C) Graph indicating the measurements of mice (n=3) across all three genotypes between the ages of 6 and 10 weeks and wild-type and P254R mice of age one year or older. Three measurements were taken from the central stack of the cornea, while four measurements were taken peripherally. One way ANOVA revealed no significant differences between genotypes.

To investigate defects in the visual signaling system in *Vsx1 P254R* mice two different approaches were taken; the first was to look at the visual signaling for any abnormalities through ERG recordings (data not shown), secondly to look at defects in the retinal bipolar cells by looking at two markers of terminal bipolar cell differentiation.

3.5.1 Immunolabeling of Vsx1 expression in Vsx1 P254R adult retinas

Using retinal sections from 6 week old wild-type, *Vsx1*-null controls and *Vsx1 P254R* mice, I performed immunolabeling for VSX1 and compared expression across the INL of the retina (n=3). Wild-type VSX1 expression is localized to the somas of the bipolar cells in the INL (Figure 11A). When VSX1 is knocked out there is complete loss of VSX1 staining is lost consistent with previous findings (Chow et al. 2004) (Figure 11C). In contrast, *Vsx1 P254R* mice showed no overt differences in expression patterns in the somas of the bipolar cells in the INL (Figure 11B). This indicates that the mutation P254R does not alter VSX1 expression or subcellular localization in the inner nuclear layer of the retina.

3.5.2 Immunolabeling and quantitation of Recoverin expression in Vsx1 P254R adult retinas

Removal of *Vsx1* shows a dual function for this transcription factor *in vivo* as both marked increase and decrease of markers has been shown (Chow et al. 2004, Shi et al. 2011). This indicates that *Vsx1* may act as a transcriptional repressor or activator *in vivo* either through direct action or indirect mechanisms.

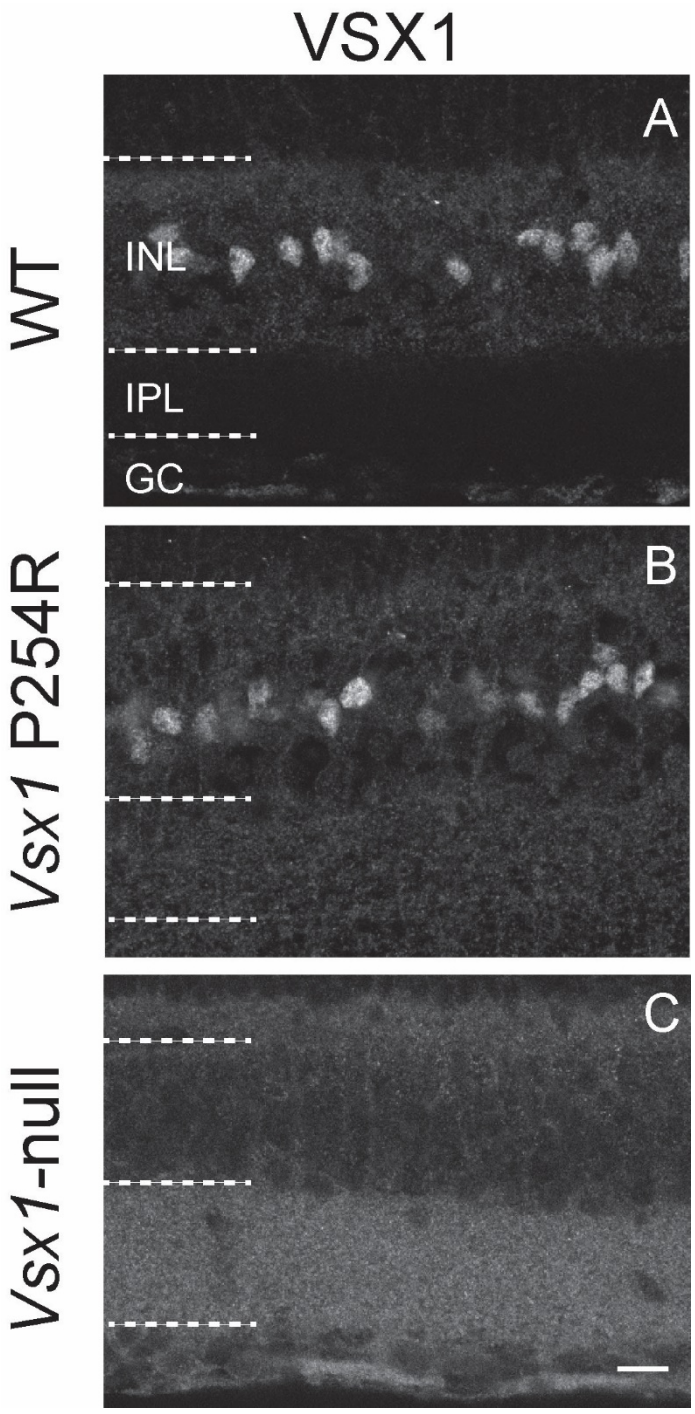

Figure 10. Immunolabeling staining of *Vsx1* reveals no changes in *Vsx1* expression in the inner retina in *Vsx1 P254R* mice when compared to wild-type expression and complete loss of expression in *Vsx1*-null mice.

(A) Representative image of Vsx1 staining in the inner nuclear layer (INL) of the mouse retina. Dotted lines indicate borders for retinal regions. Staining shows expected isolation of Vsx1 expression to the INL (B) Vsx1 staining of the P254R retina showing no changes to Vsx1 expression located in the INL. (C) Representative image of a *Vsx1*-null mouse stained for Vsx1 showing loss of expression in the INL. Scale bar indicative of 50 µm. Retinas of 6 week old mice (n=3).

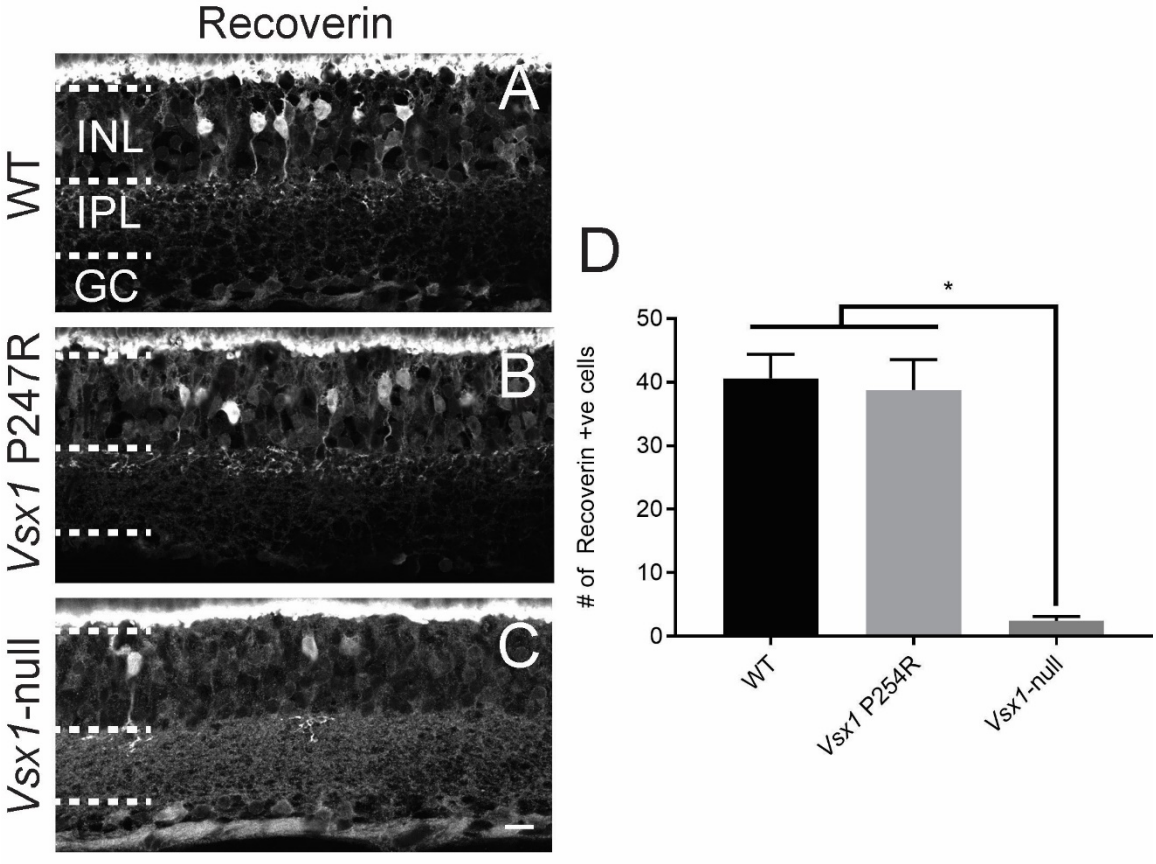

Figure 11. No change in the Type 2 cone bipolar cell marker Recoverin in *Vsx1 P254R* mice

(A) Representative image showing recoverin staining of cone bipolar cells in the INL of a wild-type mouse retina. Dotted lines delineate interfaces between layers of the retina. (B) Recoverin staining of a 6 week old *Vsx1 P254R* mouse retina. (C) Representative recoverin staining of a 6 week old *Vsx1*-null mouse showing a marked decrease in recoverin expression *in vivo*. (D) Quantitation of recoverin positive cells taken across a section of the central retina. 3 to 4 central sections and images were taken per mouse with

an n=3 of each genotype used. Cells were counted above a set threshold for fluorescence intensity. One way ANOVA revealed a significant difference in *Vsx1*-null mice with a p value of < 0.002 (Dunnett's test). No significance was found in *Vsx1 P254R* mice when compared to wild-type. Scale bar 25 µm.

I next examined expression of recoverin in the P254R retinas which is reduced in bipolar cells of the *Vsx1*-null retina (Chow et al. 2004). In wild-type retinas, recoverin expression is detected in Type 2 bipolar cells of the INL of the retina (Figure 12A). Retinas from 6 week old mice (n=3) were immunolabeled for recoverin (Figure 12 B) and using the optic nerve as a landmark (size) central portions of the retina were quantified for recoverin positive cells (One way ANOVA, dunnett's test p <0.001). Consistent with previous studies, recoverin expression in *Vsx1*-null mice (Figure 12C) showed a significant decrease in recoverin positive cells in the INL (Figure 12D). In contrast, *Vsx1 P254R* mice exhibited no differences in the number of INL recoverin positive bipolar cells compared to wild-type controls (Figure 12D).

3.5.3 Immunolabeling and quantitation of Chx10 expression in Vsx1 P254R adult retinas

In contrast to the decreased levels of recoverin seen in null controls, the opposite is observed in the expression levels of Chx10 in Vsx1 expressing Type 7 ON bipolar cells in adult retains of *Vsx1*-null mice (Shi et al. 2011). To investigate if there were any changes in Chx10 levels in *Vsx1 P254R* retinas were labeled for PKCα, Chx10 and GFP (Figure 13A-C). Type 7 ON bipolar cells are identified by being positive for GFP but negative for PKCα. In contrast rod bipolar cells are negative for GFP but positive for PKCα. Both cell types are positive for Chx10, however, in wild-type mice Type 7 Chx10 expression is significantly lower than rod bipolar expression when compared. Somas of rod bipolar cells are indicated in blue and the visible difference in Chx10 expression between cell types can be seen in wild-type retinas when compared to the Type 7 somas outlined in green (Figure 13A-C).

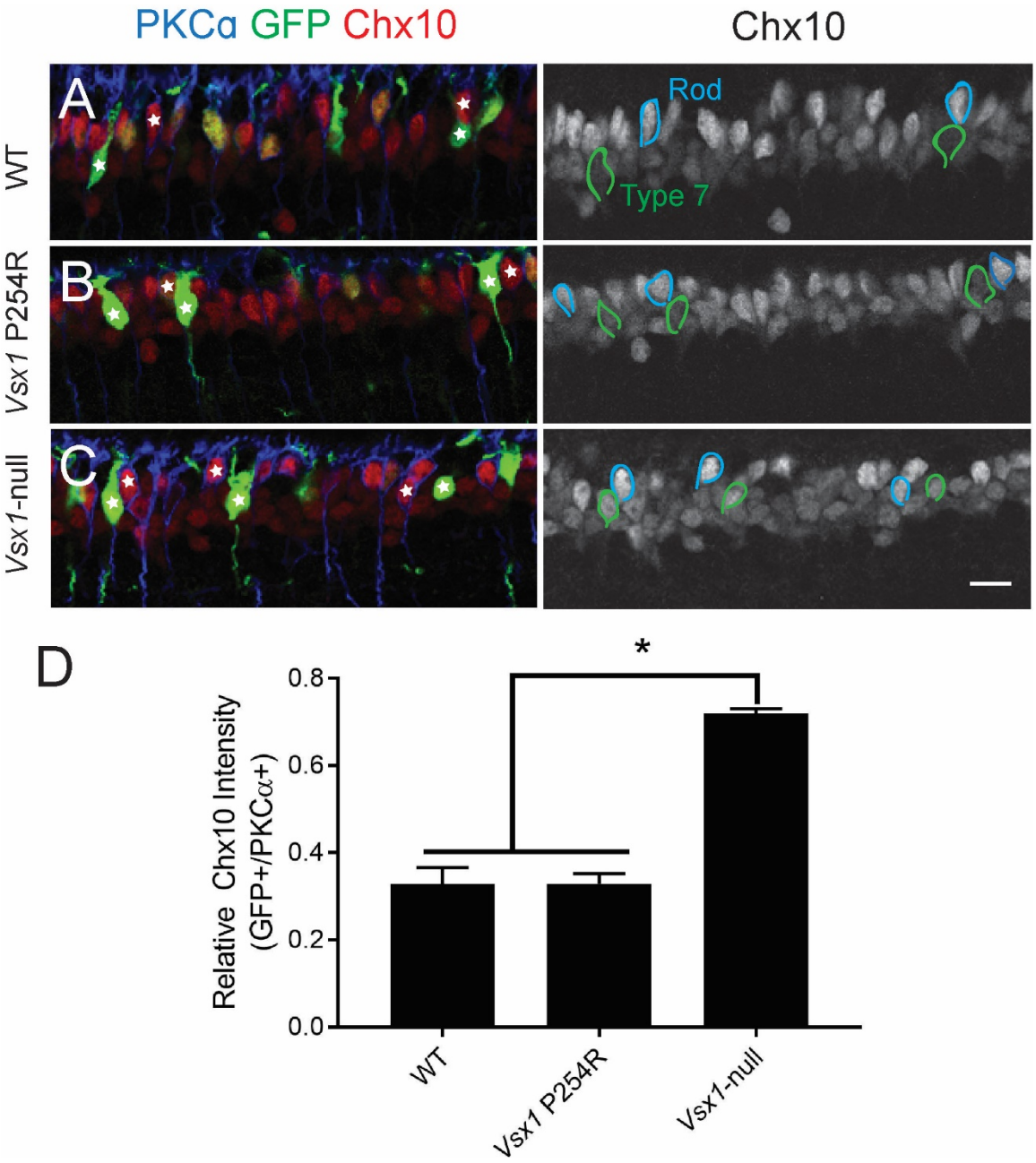

Figure 12. Quantitation of immunocytochemistry for Chx10 in Type 7 ON bipolar cells in the INL of 6 week old retinas in *Vsx1 P254R* mice compared to wild-type and null controls shows no significant differences.

(A) PKCα, GFP and Chx10 Triple labeled 6 week old retinas showing expression for Chx10 in the INL and the differential expression of Chx10 in rod bipolar cells (PKCα +ve/GFP –ve) versus Type 7 ON bipolar cells (PKCα –ve/GFP +ve). Rod bipolar somas outlined in blue, Type 7 ON bipolar somas outlined in green. (B) Triple labeled Vsx1

P254R retina showing Chx10 expression in the INL and identifying the differing bipolar cell somas (C) Vsx1-null control retina triple labeled to show differential Chx10 expression in the somas of the bipolar cells of the inner nuclear layers. Blue outlined rod bipolar cells compared to green outlined Type 7 ON somas shows a visible increase in Chx10 expression. Scale bar represents 10 µm. (D) Quantitation of Chx10 levels in the somas of Type 7 ON bipolar cells (PKCα –ve/GFP +ve) normalized to rod bipolar cell (PKCα +ve/GFP –ve) Chx10 expression levels. Significant increase in Chx10 expression in null controls when compared to wild-type controls and *Vsx1 P254R* (One way ANOVA, Dunnetts test, $p < 0.002$, n=3). No significant difference seen between *Vsx1 P254R* Chx10 expression and wild-type controls. Scale bar 10 µm.

I observed a similar significant difference in Chx10 levels when *Vsx1*-null controls were compared to wild-type retinas, as previously described (Shi et al. 2011) (One way ANOVA, Dunnett's test $p < 0.02$, n=3) (Figure 13D). However, when *Vsx1 P254R* mice were compared to wild-type controls, no significant differences were observed in the Chx10 intensity of Type 7 ON bipolar cells when normalized to the Chx10 intensity in rod bipolar cells. The lack of changes seen in recoverin expression in bipolar cells and in Chx10 expression in Type 7 ON bipolar cells indicates that *Vsx1 P254R* is not disruptive to *Vsx1* function to the same extent as in *Vsx1*-null controls and may indicate that this variant is non-pathogenic in mice *in vivo.*

Chapter 4 Discussion

Inherited diseases that affect the cornea in a progressive, bilateral and non-inflammatory manner are classified as corneal dystrophies (Weiss et al. 2015, Le et al. 2016, Valgaeren et al. 2017). A key part of classifying corneal dystrophies involves identifying genes that are pathogenic for each specific disorder and even further so, finding variants in disease populations (Weiss et al. 2015). Here, I have examined the pathogenicity of the gene *Vsx1,* which has been associated with the corneal dystrophy posterior polymorphous corneal dystrophy (PPCD) and the corneal disease keratoconus.

PPCD is an autosomal dominant endothelial dystrophy that results from morphological changes to the cells of the corneal endothelium that results in them taking on epithelial cell like properties. This leads to multi-cellular layering and a loss of the important single cell layer characteristic of the endothelium. The dystrophy presents as opacities and lesions that interfere with corneal clarity (Le et al. 2016). A second disease of interest is called keratoconus. Keratoconus results from a non-inflammatory thinning of the stromal layer of the cornea and leads to varied severity of astigmatism which can interfere with vision (Valgaeren et al. 2017). Keratoconus is not currently classified as a dystrophy as the inheritance pattern of the disease remains controversial with only about 10% of cases have positive family history and both autosomal dominant and recessive forms being reported (Weiss et al. 2015).

Studies have shown that keratoconus and PPCD may be associated as both disease can appear in one patient (Gasset and Zimmerman 1974, Weissman et al. 1989, Bechara et al. 1991, Blair et al. 1992, Driver et al. 1994, Cremona et al. 2009, Lam et al. 2010, Vincent et al. 2013). Due to this link, the search for a genetic link to these two diseases began in 1995 and in 2002 a candidate gene was chosen called *VSX1* (Héon et al. 1995, 2002). Since this time many variants have been identified in both PPCD and keratoconus disease populations, however, some variants are found in control populations, VSX1/Vsx1 has not been detected in the adult human or mouse cornea and removal of *Vsx1* in a mouse model leads no overt corneal defects and only minor defects in cone bipolar cell terminal differentiation and signal in the inner adult retina (Table 1) (Chow et al. 2004, Ohtoshi et al. 2004, Shi et al. 2011, 2012, Watson and Chow 2011). As a whole,

these findings have built controversy around the pathogenicity of mutations in *VSX1* for PPCD and keratoconus and investigations into how these mutations may affect VSX1 protein function or cornea phenotypes *in vivo* in model organisms has yet to be explored (Aldave 2005).

This study aimed to investigate the pathogenicity of *VSX1* by utilizing an extensive approach that included *in vitro* functional protein assays and the expression of one mutation *Vsx1 P254R* (*VSX1 P247R*) in a mouse model to evaluate corneal and visual signaling phenotypes *in vivo* in relation to mutations found in keratoconus and PPCD disease populations.

4.1 Seven *VSX1* missense mutations result in changes to transcriptional activity *in vitro* but do not alter protein expression or subcellular localization

Determining the pathogenicity of *VSX1* in PPCD keratoconus populations not only requires the identification of mutations in affected patients but verification of their effects on *VSX1* function through protein functional assays is necessary as well (Aldave 2005). Presently, the bulk of research surrounding the role of *VSX1* in corneal disease has been lacking a thorough investigation into how *VSX1* mutations may lead to disease phenotypes. Two studies exist that examined the transcriptional activity of *VSX1* R166W and its expression levels *in vitro*. These authors found that not only does VSX1 act as a transcriptional repressor *in vitro* but that R166W disrupts the binding strength and transcriptional repression of VSX1 (Héon et al. 2002, Dorval et al. 2005). Through my approach I aimed to characterize how *Vsx1* mutations in the homeodomain and CVC effect protein function, expression and localization. These aspects were studied by an *in vitro* transcriptional activity assay, western blotting and subcellular localization assays respectively.

To investigate how *Vsx1* transcriptional repressor activity was affected when mutated with VSX1 mutants I designed a Gal4 based repressor activity assay. Consistent with previous findings, when VSX1 is introduced reporter activity is attenuated indicating VSX1 functioning as a transcriptional repressor. My findings revealed that five out of the seven *Vsx1* mutations examined, R173W, Q182H, G246R, H251R and P254R, trended towards an increase in transcriptional repression with at least four of them

showing 1.5 times stronger repressive function. Interestingly, the R223H mutation found in the homeodomain showed a complete loss of transcriptional repression (p 0.0002, n=5). The final mutation, A263S, located in the CVC domain showed no significant change in activity when compared to wild-type protein.

To further investigate the changes in *V*sx1 transcriptional activity observed in the luciferase reporter experiments, I investigated whether they may have arisen from changes in expression levels. Utilizing western blotting of protein lysates from HEK cells transfected with different *Vsx1* mutation expression constructs. No significant differences in expression levels across all described mutations was observed in comparison to wild-type Vsx1. Furthermore, wild-type Vsx1 showed a normal subcellular localization pattern that was restricted to the nucleus and none of the seven mutations expressed disrupted this expression pattern.

It is important when considering effects mutations may have on *Vsx1* function to consider all three parts of our *in vitro* analysis as a whole. This is the first study to show that mutations spanning both the homeodomain and CVC domain can alter transcriptional activity in *Vsx1*. The effect these mutations have on functional activity do not change protein expression or subcellular localization removing these as possibilities for the observed change in repression. Transcription homeodomains exert their main functional activity by binding to DNA and are known to have many protein-protein interactions that contribute to and modulate their function (Kurtzman et al. 2000, Kurtzman and Schechter 2001, Dorval et al. 2005). Both of these features could be altered in the case of our mutations as these would not be seen when looking at changes in expression or localization. This is especially interesting in the case of the CVC domain whose domain has remained unknown up until this point. Although my activity assay does not conclusively establish the function of the CVC domain, it does suggest that even though the homeodomain is the main DNA binding domain of the protein, the CVC domain may play a role in DNA binding and repressor activity of *VSX1* or may be contributing to protein-protein interactions that alter activity that are disrupted when mutations are introduced. Taken into account with the changes in activity seen in the homeodomain mutations, it is possible that both the homeodomain and CVC domain may be involved in

the DNA binding function and the mutations are causing conformational changes that result in the increase in transcriptional repression.

The loss of transcriptional repression seen with the R223H mutation may be explained by the nature of this missense change. This change causes a charged amino acid, arginine, to be replaced with the bulk ring structure of a histidine residue. This may have large implications in conformational changes in that portion of the protein. R223H is located in the recognition helix of the homeodomain and resides at an arginine residue highly conserved throughout all homeodomains and whose function is pivotal to proper DNA binding (Shang et al. 1994, Chi 2005). The location of this residue in not only the recognition helix but as well as a known "hot spot" residue for mutation could explain why any disruptions to protein structure, due to the histidine change, could remove the ability of the protein to bind to DNA (Chi 2005). As with the changes seen in the other mutations, it is possible that, in addition to disrupting DNA binding, the R223H mutation could be causing changes in protein-protein interactions that result in null activity rather in contrast to the increase in repressor activity we have seen with the other variants.

Due to the fact that we used the mouse sequence in our expression constructs and not the human constructs, we cannot rule out that there may be differences in transcriptional activity in the human sequence as well as differences in the interactome of VSX1. Although, the sequence between both the homeodomain and the CVC domain in humans and mice is highly conserved with only six changes overall (Héon et al. 2002, Chow et al. 2004) (Figure 3) and these domains are the location of our mutations, it is reasonable to expect similar results with the human sequence in place.

The most interesting implication from these results comes from the knowledge that transcription factors do interact heavily with other proteins and these interactions have a large influence on how the transcription factor interacts with its targets (Kurtzman and Schechter 2001). The debate around whether *VSX1* mutations are pathogenic for corneal diseases may be explained due to the fact that the mutations themselves are not obliterating *VSX1* activity or even changing its activity directly. These mutations, as previously mentioned, could be directly changing the interactions *VSX1* makes with other proteins possibly causing disruption or increasing interaction strengths which would mean other factors not yet identified are involved in the pathogenicity of these diseases.

The results of my transcriptional activity assay would lend well to investigating changes in binding strength between *VSX1* and its targets between wild-type and mutated protein. Also these results encourage further discovery studies into the targets of *VSX1* as well as the proteins *VSX1* interacts with. Additionally, discerning the conformational structure of *VSX1* would be valuable in looking into how each one of these mutations, especially the R223H mutation, may change the protein conformation and in turn the function of *VSX1*.

4.2 Interpreting the role of *Vsx1 P254R in vivo*

For both PPCD and keratoconus, their disease phenotypes vary in severity depending on the patient and both diseases are slow in their progression (Weiss et al. 2015). These disease characteristics make studying PPCD and keratoconus difficult and may contribute to the difficulties in understanding genetic factors contributing to their phenotypes. With both being slowly progressive this also presents a unique hurdle to overcome in studying these disorders in *in vivo* models. As previously discussed, 20 variants in *VSX1* associated with PPCD and keratoconus have been identified since the initial candidate gene selection in 2002 (Table 1, Héon et al. 2002). However, there has been no cohesive conclusion made amongst all of these studies as some conclude variants are pathogenic, while others conclude pathogenicity is unfounded and many may in fact be benign polymorphisms (Aldave et al. 2005, Dash et al. 2010, Shetty et al. 2015). The ability to study diseases in *in vivo* models aids greatly in understanding causative factors of the disease as well as assessing disease phenotypes and progression. No *in vivo* model exists for either PPCD or keratoconus, however, expressing *VSX1* mutations in a mouse may lead to insights into how *VSX1* may or may not contribute to their phenotypes and could help sort out the controversy surrounding *VSX1* pathogenicity leading to a confirmation of this link or leading to a search for new causative factors.

In this study I wanted to express one of these intriguing mutations in a mouse model to evaluate the effects of corneal cellular morphology, thickness and curvature *in vivo*. To do this, using CRISPR genome editing technology, I introduced the *VSX1* variant P247R which in mice is the variant P254R. This missense change results from a highly conserved proline residue, which is often responsible for creating turns in protein

structure, being replaced with a charged arginine reside. The nature of this mutation has large implications for protein structure changes and possible changes in crucial structure involved in function and interactions *Vsx1* requires proper transcriptional activity. I designed a new methodology for *ex vivo* whole eye confocal microscopy that coupled the power of confocal imaging with a membrane bound dye to visualize corneal curvature, thickness and cellular morphology in whole eye live tissue. Additionally, I carried out histological analysis on corneas to look for changes to cellular morphology in the corneal epithelium, stroma and endothelium. Corneas from adult P254R mice ranging from 6 to 10 weeks of age were evaluated against wild-type and null controls as well as mice kept long term for at least a year to address the progressive nature of PPCD and keratoconus.

Utilizing the membrane dye, I was able to take images in stack throughout the whole cornea to obtain a projection that represented the outer curvature of the cornea and could be evaluated for astigmatism changes characteristic to the disease keratoconus. Additionally, stack images were taken through the thickness of the cornea in a central region after the introduction of a dye into small incision in the limbal region. This allowed me to reconstruct a maximum projection that represented the thickness of a 50 µm central portion of the cornea and also allowed me to look at cellular morphology through the three cellular layers of the cornea as I stepped down through the anterior to posterior cornea. Additionally, corneas from the same mice used for confocal imaging were used to obtain histological sections that were then imaged to look at corneal morphology of fixed corneas.

In analyzing the corneal thickness of mice across genotypes, measurements were isolated for the peripheral cornea and the central cornea as in mice there are natural differences in thickness as you move peripherally. Corneal thickness measurements show no significant differences in *Vsx1 P254R* mice when compared to wild-type and *Vsx1*-null controls in 6 to 10 week old animals. Furthermore, long term *Vsx1 P254R* mice used for analysis at, at least a year of age, revealed no significant differences in thickness when compared to wild-type mice of the same age. Corneas sent for histological sectioning were assessed for changes in corneal morphology to the epithelium, stroma and most importantly the endothelium to look for characteristic changes known to be clinically present in patients with keratoconus and PPCD. Imaging across the whole

cornea revealed no overt changes to the corneal endothelium, such as multicellular layering, classically representative of PPCD in humans. Epithelial and stromal cell layers of P254R mice of age 6 to 10 weeks and of a year or older when compared to wild-type mice also revealed no observable changes.

Due to the absence of phenotypic changes in corneal curvature, thickness, and cellular morphology I concluded that *Vsx1 P254R* is not pathogenic for PPCD or keratoconus in our mouse model. However, the absence of a phenotype is intriguing in itself. As previously mentioned, the debate around the pathogenicity of *VSX1* continues on, and the search for other causative factors has yet to definitively find any other promising candidates. From our *in vitro* functional assays, the P254R mutation trends towards increased transcriptional repression, this change may not be disease causing on its own. However, the *in vitro* findings coupled with our analysis *in vivo* may support the idea that these disease are multi-factorial and other proteins interacting with *VSX1* may be involved. Additionally, this could be indicative of the lack of pathogenicity in *VSX1* and may be the evidence needed to put the pathogenicity debate of *VSX1* to rest and put forth those efforts into finding other genetic factors that might be involved.

These findings however do not completely rule out the role of *VSX1* in corneal dystrophies and diseases. As we only expressed one other mutation in mice, it would be of interest to express other mutations found in the homeodomain and CVC domain of *VSX1* that show more overt changes to transcriptional repression, especially the R223H mutation that appears to act a null mutation for *VSX1* activity. Furthermore, mutations outside these two functional domains have also been identified and depending on the conservation of each of the residues, looking into the functional implications of these mutations *in vitro* and possibly their pathogenicity in an *in vivo* model much like ours could lend valuable insight into the field of work surrounding this topic.

4.3 Evaluating the requirement of *Vsx1* in the visual system in the *in vivo Vsx1 P254R* mouse model

Previous studies have investigated the implication of removing *VSX1 in vivo* in the *Vsx1*-null mouse and these studies have revealed the requirement for its presence and proper function in the visual system (Chow et al. 2004, Ohtoshi et al. 2004, Shi et al.

2011, 2012). More specifically these studies have shown a requirement for *Vsx1* in the terminal differentiation and proper visual signaling of the cone bipolar cells of the inner adult retina (Chow et al. 2004, Ohtoshi et al. 2004, Shi et al. 2011, 2012). Moreover, these mice lack phenotypic changes in the adult cornea. Both the cells of the retina and the portions of the cornea arise from the same ectoderm cells during development (Lwigale 2015). With this knowledge, investigating visual signaling defects in the *Vsx1 P254R* mice was pivotal for understanding the role this mutation, and possibly other mutations associated with corneal dystrophies, play in the mouse model and may indicate dysfunction not uncovered by just investigating the adult cornea.

Studies done in *Vsx1*-null mice show defects in the terminal differentiation of the bipolar cells of the inner retina (Chow et al. 2004, Shi et al. 2011, 2012). As previously discussed, two of these markers are recoverin and Chx10 and *in vivo* have opposing phenotypes as recoverin expression drastically decreases across the majority of bipolar cells while Chx10 expression levels show a significant increase in the Type 7 ON bipolar cells (Chow et al. 2004, Shi et al. 2011). In contrast, our *Vsx1 P254R* mice showed no significant changes to recoverin expression. Similarly, when Chx10 levels were quantitated in the Type 7 ON bipolar cells of the inner retina and normalized to levels in rod bipolar cells, null controls showed the expected increase in expression levels while my *Vsx1 P254R* mice showed no significant differences in levels of Chx10 in these cells when compared to wild-type controls.

Together these findings lend more support to P254R not being pathogenic *in vivo* and possibly not being pathogenic for corneal dystrophies in humans. However, as this is only one mutation found in disease populations and has been found in unaffected controls in human studies, this does not rule out the pathogenicity for mutations in VSX1 for PPCD and keratoconus all together and requires further investigation into the other mutations located in the homeodomain and CVC domain of the protein and possibly the mutations outside of the functional domains.

4.4 Conclusions and future directions for the implications of *Vsx1* mutations *in vitro* and *Vsx1 P254R in vivo*

My thesis work has shown the implications of mutations associated with the corneal dystrophy, posterior polymorphous corneal dystrophy and the corneal disease keratoconus. Through this work I showed that mutations, found in disease populations, spanning the homeodomain and the CVC domain have the ability to disrupt the transcriptional repressive activity of *Vsx1 in vitro* with five mutations studied showing an increase in activity and one mutation removing VSX1 repression all together. However, I have shown that these mutations do not alter *Vsx1* expression or subcellular localization *in vitro*. In addition to my findings *in vitro* my *in vivo* investigation of the *Vsx1 P254R* mouse looked at cornea cellular morphology, thickness and curvature and the requirement of *Vsx1* in the visual signaling system and revealed no overt phenotypes in these areas when compared to wild-type and *Vsx1*-null controls.

This study can be marked as the first of its kind in the field of corneal dystrophies and contributes valuable information to the ongoing controversy surrounding the pathogenic link between *VSX1* and PPCD and keratoconus. With that, this work lends well to a variety of future studies. These include further investigation into the changes seen in transcriptional repression. As previously mentioned, although no changes were since in the protein expression or subcellular localization, these mutations could be altering the binding activity of the protein itself or the protein-protein interactions that are indeed pivotal for the proper function of *VSX1*.

Even though no significant differences were seen *in vivo* in the *Vsx1 P254R* mouse, there is still much to be known about the role of *Vsx1* in *in vivo* models. Future studies conducted in this area must further look into how other mutations associated with PPCD and keratoconus in disease populations might present in a mouse model. Additionally, though *VSX1* is not expressed in the cornea itself, there are other areas of expression that could exist that may possibly result in corneal phenotypes. Areas may exist in the ophthalmic branch of the trigeminal ganglia which is responsible for the innervation of the cornea, which is interestingly one of the most highly innervated tissues in the body. These studies could include looking for *VSX1* expression itself in the trigeminal ganglia (unpublished data, Peter Watson) as well as looking at feedback

mechanisms and secretory pathways between the nerves innervating the cornea and cornea tissues itself. Of course, my investigation in the P254R mouse also lends evidence for *VSX1* not being pathogenic for this variant specifically but could be insight into the pathogenicity for identified variants overall. PPCD and keratoconus are known to be genetically heterogeneous (Le et al. 2016, Valgaeren et al. 2017) and *VSX1* possibly could not be pathogenic on its own as other factors could be involved in the disease mechanism. Future studies should also include the search for new genetic factors that interact with *VSX1*, as protein-protein interactions have already been shown to be important for proper localization of *VSX1* (Kurtzman and Schechter 2001) and could be contributing to disease phenotypes. Additional studies should involve the search for new genetic candidates all together. Further analysis is also required to look at possible changes to corneal curvature and visual signaling pathways through ERG, in our *Vsx1 P254R* mice

In summary this study was the first of its kind to approach the controversy of *VSX1* pathogenicity utilizing both an *in vitro* approach to functional protein assays and an *in vivo* approach utilizing a model organism, in this case a mouse, to assess the pathogenicity of a *VSX1* mutation associated with PPCD and keratoconus. Most importantly, this study highlighted that mutations found in the homeodomain and the CVC domain can affect the transcriptional activity of *VSX1* and therefore lends evidence that *VSX1* may still be pathogenic for corneal disease and more specifically PPCD and keratoconus *in vivo*.

Bibliography

Aldave, A.J. 2005. VSX1 Mutation and Corneal Dystrophies Letter to the Editor. Ophthalmology **112**(1): 170–171.

Aldave, A.J., Yellore, V.S., Principe, A.H., Abedi, G., Merrill, K., Chalukya, M., Small, K.W., and Udar, N. 2005. Candidate gene screening for posterior polymorphous dystrophy. Cornea **24**(2): 151–5. doi:00003226-200503000-00005 [pii].

Aldave, A.J., Yellore, V.S., Salem, A.K., Yoo, G.L., Rayner, S.A., Yang, H., Tang, G.Y., Piconell, Y., and Rabinowitz, Y.S. 2006. No VSX1 gene mutations associated with keratoconus. Investig. Ophthalmol. Vis. Sci. **47**(7): 2820–2822. doi:10.1167/iovs.05-1530.

Ambati, B.K., Nozaki, M., Singh, N., Takeda, A., Jani, P.D., Suthar, T., Albuquerque, R.J.C., Richter, E., Sakurai, E., Newcomb, M.T., Kleinman, M.E., Caldwell, R.B., Lin, Q., Ogura, Y., Orecchia, A., Samuelson, D.A., Agnew, D.W., St. Leger, J., Green, W.R., Mahasreshti, P.J., Curiel, D.T., Kwan, D., Marsh, H., Ikeda, S., Leiper, L.J., Collinson, J.M., Bogdanovich, S., Khurana, T.S., Shibuya, M., Baldwin, M.E., Ferrara, N., Gerber, H.P., De Falco, S., Witta, J., Baffi, J.Z., Raisler, B.J., and Ambati, J. 2006. Corneal avascularity is due to soluble VEGF receptor-1. Nature **443**(7114): 993–997. doi:10.1038/nature05249.

Bechara, S.J., Grossniklaus, H.E., Waring, G.O., and Wells, J.A. 1991. Keratoconus Associated with Posterior Polymorhpus Dystrophy. Am. J. Opthalmology **112**(6): 729–731.

Bendl, J., Stourac, J., Salanda, O., Pavelka, A., Wieben, E.D., Zendulka, J., Brezovsky, J., and Damborsky, J. 2014. PredictSNP: Robust and Accurate Consensus Classifier for Prediction of Disease-Related Mutations. PLoS Comput. Biol. **10**(1): 1–11. doi:10.1371/journal.pcbi.1003440.

Bisceglia, L., Ciaschetti, M., De Bonis, P., Alberto, P., Campo, P., Pizzicoli, C., Scala, C., Grifa, M., Ciavarella, P., Noci, N.D., Vaira, F., Macaluso, C., and Zelante, L. 2005. VSX1 Mutational Analysis in a Series of Italian Patients Affected by Keratoconus: Detection of a Novel Mutation. Invest Ophthalmol Vis Sci **46**: 39–45. doi:10.1167/iovs.04-0533.

Blair, S.D., Seabrooks, D., Shields, W.J., Pillai, S., and Cavanagh, H.D. 1992. Bilateral Progressive Essential Iris Atrophy and Keratoconus with Coincident Features of Posterior Polymorphous Dystrophy: A Case Report and Proposed Pathogenesis. Cornea **11**(3): 255–261.

De Bonis, P., Laborante, A., Pizzicoli, C., Stallone, R., Barbano, R., Longo, C., Mazzilli, E., Zelante, L., and Bisceglia, L. 2011. Mutational screening of VSX1, SPARC, SOD1, LOX, and TIMP3 in keratoconus. Mol. Vis. **17**(July): 2482–94. doi:269 [pii].

Bremner, R., Cohen, B.L., Sopta, M., Hamel, P.A., Ingles, C.J., Gallie, B.L., and Phillips, R.A. 1995. Direct transcriptional repression by pRB and its reversal by specific cyclins. Mol. Cell. Biol. **15**(6): 3256–65. Available from http://www.pubmedcentral.nih.gov/articlerender.fcgi?artid=230558&tool=pmcentrez&rendertype=abstract.

Chang, H.Y.P., and Chodosh, J. 2013. The genetics of keratoconus. Semin. Ophthalmol. **28**(5–6): 275–280. doi:10.3109/08820538.2013.825295.

Chaurasia, S., Mittal, R., Bichappa, G., Ramappa, M., and Murthy, S.I. 2017. Clinical characterization of posterior polymorphous corneal dystrophy in patients of Indian ethnicity. Int. Ophthalmol. **37**(4): 945–952. Springer Netherlands. doi:10.1007/s10792-016-0360-y.

Chi, Y.-I. 2005. Homeodomain Revisited: a Lesson from Disease-causing Mutations. Hum. Genet. **116**(6): 433–444. doi:10.1080/10810730902873927.Testing.

Chow, R.L., Snow, B., Novak, J., Looser, J., Freund, C., Vidgen, D., Ploder, L., and McInnes, R.R. 2001. Vsx1, a rapidly evolving paired-like homeobox gene expressed in cone bipolar cells. Mech. Dev. **109**(2): 315–322. doi:10.1016/S0925-4773(01)00585-8.

Chow, R.L., Volgyi, B., Szilard, R.K., Ng, D., McKerlie, C., Bloomfield, S. a, Birch, D.G., and McInnes, R.R. 2004. Control of late off-center cone bipolar cell differentiation and visual signaling by the homeobox gene Vsx1. Proc Natl Acad Sci U S A **101**(6): 1754–1759. doi:10.1073/pnas.0306520101.

Chung, D.D., Frausto, R.F., Cervantes, A.E., Gee, K.M., Zakharevich, M., Hanser, E.M., Stone, E.M., Heon, E., and Aldave, A.J. 2017. Confirmation of the OVOL2 Promoter Mutation c.-307T>C in Posterior Polymorphous Corneal Dystrophy 1. PLoS One **12**(1): 1–11. doi:10.1371/journal.pone.0169215.

Collomb, E., Yang, Y., Foriel, S., Cadau, S., Pearton, D.J., and Dhouailly, D. 2013. The corneal epithelium and lens develop independently from a common pool of precursors. Dev. Dyn. **242**(5): 401–413. doi:10.1002/dvdy.23925.

Cremona, F.A., Ghosheh, F.R., Rapuano, C.J., Eagle, R.C., Hammersmith, K.M., Laibson, P.R., Ayres, B.D., and Cohen, E.J. 2009. Keratoconus associated with other corneal dystrophies. Cornea **28**(2): 127–135. doi:10.1097/ICO.0b013e3181859935.

Dash, D.P., George, S., O'Prey, D., Burns, D., Nabili, S., Donnelly, U., Hughes, a E., Silvestri, G., Jackson, J., Frazer, D., Héon, E., and Willoughby, C.E. 2010. Mutational screening of VSX1 in keratoconus patients from the European population. Eye (Lond). **24**: 1085–1092. doi:10.1038/eye.2009.217.

DelMonte, D.W., and Kim, T. 2015. Anatomy and physiology of the cornea. Keratoprostheses Artif. Corneas Fundam. Surg. Appl. **37**(3): 19–25. ASCRS and ESCRS. doi:10.1007/978-3-642-55179-6_3.

Dhouailly, D., Pearton, D.J., and Michon, F. 2014. The vertebrate corneal epithelium: From early specification to constant renewal. Dev. Dyn. **243**(10): 1226–1241. doi:10.1002/dvdy.24179.

Dorval, K.M., Bobechko, B.P., Ahmad, K.F., and Bremner, R. 2005. Transcriptional activity of the paired-like homeodomain proteins CHX10 and VSX1. J. Biol. Chem. **280**(11): 10100–10108. doi:10.1074/jbc.M412676200.

Driver, P.J., Reed, J.W., and Davis, R.M. 1994. Familial Cases of Keratoconus Associated with Posterior Polymorphous Dystrophy. Am. J. Opthalmology **118**(2): 256–257.

Edwards, M., McGhee, C.N., and Dean, S. 2001. The genetics of keratoconus. Clin. Exp. Ophthalmol. **29**: 345–351.

Eghrari, A.O., Riazuddin, S.A., and Gottsch, J.D. 2015. Overview of the Cornea: Structure, Function, and Development. *In* Progress in Molecular Biology and Translational Science, 1st edition. Elsevier Inc. doi:10.1016/bs.pmbts.2015.04.001.

Eran, P., Almogit, A., David, Z., Wolf, H.R., Hana, G., Yaniv, B., Elon, P., and Isaac, A. 2008. The D144E substitution in the VSX1 gene: A non-pathogenic variant or a disease causing mutation? Ophthalmic Genet. **29**(2): 53–59. doi:10.1080/13816810802008242.

Eran, P., Almogit, A., David, Z., Wolf, H.R., Hana, G., Yaniv, B., Elon, P., Isaac, A., Eran, P., Almogit, A., David, Z., Wolf, H.R., Hana, G., Yaniv, B., Elon, P., Isaac, A., Substitution, T.D.E., and Gene, V.S.X. 2009. The D144E Substitution in the VSX1 Gene : A Non- pathogenic Variant or a Disease Causing Mutation ? The D144E Substitution in the VSX1 Gene : A Non-pathogenic Variant or a Disease Causing Mutation ? **6810**. doi:10.1080/13816810802008242.

Gasset, A.R., and Zimmerman, T.J. 1974. Posterior Polymorhpous Dystrophy Associated with Keratoconus. Am. J. Opthalmology **78**(3): 535–537.

He, J., and Bazan, H.E.P. 2016. Neuroanatomy and neurochemistry of mouse cornea. Investig. Ophthalmol. Vis. Sci. **57**(2): 664–674. doi:10.1167/iovs.15-18019.

Henriksson, J.T., McDermott, A.M., and Bergmanson, J.P.G. 2009. Dimensions and morphology of the cornea in three strains of mice. Investig. Ophthalmol. Vis. Sci. **50**(8): 3648–3654. doi:10.1167/iovs.08-2941.

Héon, E., Greenberg, A., Kopp, K.K., Rootman, D., Vincent, A.L., Billingsley, G., Priston, M., Dorval, K.M., Chow, R.L., McInnes, R.R., Heathcote, G., Westall, C., Sutphin, J.E., Semina, E., Bremner, R., and Stone, E.M. 2002. VSX1: a gene for posterior polymorphous dystrophy and keratoconus. Hum. Mol. Genet. **11**(9): 1029–1036. doi:10.1093/HMG/11.9.1029.

Héon, E., Mathers, W.D., Alward, L.M.A., Weisenthal, R.W., Sunden, S.L.F., Fishbaugh, J.A., Taylor, C.M., Krachmer, J.H., Sheffield, V.C., and Stone, E.M. 1995. Linkage of posterior polymorphous corneal dystrophy to 20q11. Hum. Mol. Genet. **4**(3): 485–488. doi:10.1093/hmg/4.3.485.

Hosseini, S.M., Herd, S., Vincent, A.L., and Héon, E. 2008. Genetic analysis of chromosome 20-related posterior polymorphous corneal dystrophy: genetic heterogeneity and exclusion of three candidate genes. Mol. Vis. **14**(December 2007): 71–80. doi:v14/a9 [pii].

JACOBSEN, I.E., JENSEN, O.A., and PRAUSE, J.U. 1984. STRUCTURE AND COMPOSITION OF BOWMAN'S MEMBRANE: Study by frozen resin cracking. Acta Ophthalmol. **62**(1): 39–53. doi:10.1111/j.1755-3768.1984.tb06755.x.

Jeoung, J.W., Kim, M.K., Park, S.S., Kim, S.Y., Ko, H.S., Wee, W.R., and Lee, J.H. 2012. VSX1 gene and keratoconus: Genetic analysis in Korean patients. Cornea **31**(7): 746–750. doi:10.1097/ICO.0b013e3181e16dd0.

Joyce, N.C. 2003. Proliferative capacity of the corneal endothelium. Prog. Retin. Eye Res. **22**(3): 359–389. doi:10.1016/S1350-9462(02)00065-4.

Knauer, S.K., Carra, G., and Stauber, R.H. 2005. Nuclear export is evolutionarily conserved in CVC paired-like homeobox proteins and influences protein stability, transcriptional activation, and extracellular secretion. Mol Cell Biol **25**(7): 2573–2582. doi:Doi 10.1128/Mcb.25.7.2753-2582.2005.

Kurtzman, A.L., Gregori, L., Haas, A.L., and Schechter, N. 2000. Ubiquitination and Degradation of the Zebrafish Paired -Like Homeobox Protein Vsx-1.

Kurtzman, a L., and Schechter, N. 2001. Ubc9 interacts with a nuclear localization signal and mediates nuclear localization of the paired-like homeobox protein Vsx-1

independent of SUMO-1 modification. Proc. Natl. Acad. Sci. U. S. A. **98**(10): 5602–5607. doi:10.1073/pnas.101129698.

Lam, H.Y., Wiggs, J.L., and Jurkunas, U. V. 2010. Unusual presentation of presumed posterior polymorphous dystrophy associated with iris heterochromia, band keratopathy, and keratoconus. Cornea **29**(10): 1180–1185. doi:10.1097/ICO.0b013e3181d007e1.

Le, D.J., Chung, D.W.D., Frausto, R.F., Kim, M.J., and Aldave, A.J. 2016. Identification of potentially pathogenic variants in the posterior polymorphous corneal dystrophy 1 locus. PLoS One **11**(6): 1–13. doi:10.1371/journal.pone.0158467.

Levine, E.M., Passini, M., Hitchcock, P.F., Glasgow, E., and Schechter, N. 1997. Vsx-1 and Vsx-2: Two Chx10-like homeobox genes expressed in overlapping domains in the adult goldfish retina. J. Comp. Neurol. **387**(3): 439–448. doi:10.1002/(SICI)1096-9861(19971027)387:3<439::AID-CNE9>3.0.CO;2-1.

Liskova, P., Ebenezer, N.D., Hysi, P.G., Gwilliam, R., and El-, M.F. 2017. Molecular analysis of the VSX1 gene in familial keratoconus. : 1887–1891.

Lu, Y., Vitart, V., Burdon, K.P., Khor, C.C., Bykhovskaya, Y., Mirshahi, A., Hewitt, A.W., Koehn, D., Hysi, P.G., Ramdas, W.D., Zeller, T., Vithana, E.N., Cornes, B.K., Tay, W.T., Tai, E.S., Cheng, C.Y., Liu, J., Foo, J.N., Saw, S.M., Thorleifsson, G., Stefansson, K., Dimasi, D.P., Mills, R.A., Mountain, J., Ang, W., Hoehn, R., Verhoeven, V.J.M., Grus, F., Wolfs, R., Castagne, R., Lackner, K.J., Springelkamp, H., Yang, J., Jonasson, F., Leung, D.Y.L., Chen, L.J., Tham, C.C.Y., Rudan, I., Vatavuk, Z., Hayward, C., Gibson, J., Cree, A.J., MacLeod, A., Ennis, S., Polasek, O., Campbell, H., Wilson, J.F., Viswanathan, A.C., Fleck, B., Li, X., Siscovick, D., Taylor, K.D., Rotter, J.I., Yazar, S., Ulmer, M., Li, J., Yaspan, B.L., Ozel, A.B., Richards, J.E., Moroi, S.E., Haines, J.L., Kang, J.H., Pasquale, L.R., Allingham, R.R., Ashley-Koch, A., Mitchell, P., Wang, J.J., Wright, A.F., Pennell, C., Spector, T.D., Young, T.L., Klaver, C.C.W., Martin, N.G., Montgomery, G.W., Anderson, M.G., Aung, T., Willoughby, C.E., Wiggs, J.L., Pang, C.P., Thorsteinsdottir, U., Lotery, A.J., Hammond, C.J., Van Duijn, C.M., Hauser, M.A., Rabinowitz, Y.S., Pfeiffer, N., MacKey, D.A., Craig, J.E., MacGregor, S., and Wong, T.Y. 2013. Genome-wide association analyses identify multiple loci associated with central corneal thickness and keratoconus. Nat. Genet. **45**(2): 155–163. doi:10.1038/ng.2506.

Lwigale, P.Y. 2015. Corneal Development: Different Cells from a Common Progenitor. *In* Progress in Molecular Biology and Translational Science, 1st edition. Elsevier Inc. doi:10.1016/bs.pmbts.2015.04.003.

Mazzotta, C., Baiocchi, S., Caporossi, O., Buccoliero, D., Casprini, F., Caporossi, A., and Balestrazzi, A. 2008. Confocal microscopy identification of keratoconus associated with posterior polymorphous corneal dystrophy. J. Cataract Refract. Surg. **34**(2): 318–321. doi:10.1016/j.jcrs.2007.09.028.

Mendoza-Adam, G., Hernandez-Camarena, J.C., and Valdez-García, J.E. 2015. Posterior polymorphous dystrophy, case report and literature review | Distrofia polimorfa posterior, presentación de un caso y análisis de la literatura. Arch. Soc. Esp. Oftalmol. **90**(9): 439–441. SEGO. doi:10.1016/j.oftal.2015.01.003.

Mintz-Hittner, H.A., Semina, E. V., Frishman, L.J., Prager, T.C., and Murray, J.C. 2004. VSX1 (RINX) mutation with craniofacial anomalies, empty sella, corneal

endothelial changes, and abnormal retinal and auditory bipolar cells. Ophthalmology **111**(4): 828–836. doi:10.1016/j.ophtha.2003.07.006.

Mintz-Hittner, H., and Semina, E. 2005. Vsx1 Mutation and Corneal Dystrophies Letter to the Editor: Author reply. Ophthalmology **112**(1): 171–172.

Mok, J.W., Baek, S.J., and Joo, C.K. 2008. VSX1 gene variants are associated with keratoconus in unrelated Korean patients. J. Hum. Genet. **53**(9): 842–849. doi:10.1007/s10038-008-0319-6.

Naderan, M., Rajabi, M.T., Zarrinbakhsh, P., Naderan, M., and Bakhshi, A. 2016. Association between Family History and Keratoconus Severity. Curr. Eye Res. **41**(11): 1414–1418. Taylor & Francis. doi:10.3109/02713683.2015.1128553.

Ohtoshi, A., Wang, S.W., Maeda, H., Saszik, S.M., Frishman, L.J., and Behringer, R.R. 2004. Regulation of Retinal Cone Bipolar Cell Differentiation and Photopic Vision by the CVC Homeobox Gene Vsx1. Curr. Biol. **14**: 530–536. doi:10.1016/j.

Paliwal, P., Singh, A., Tandon, R., Titiyal, J.S., and Sharma, A. 2009. A novel VSX1 mutation identified in an individual with keratoconus in India. Mol. Vis. **15**(November): 2475–9. doi:264 [pii].

Saee-Rad, S., Hashemi, H., Miraftab, M., Noori-Daloii, M.R., Chaleshtori, M.H., Raoofian, R., Jafari, F., Greene, W., Fakhraie, G., Rezvan, F., and Heidari, M. 2011. Mutation analysis of VSX1 and SOD1 in Iranian patients with keratoconus. Mol. Vis. **17**(November): 3128–36. doi:337 [pii].

Semina, E. V, Mintz-Hittner, H. a, and Murray, J.C. 2000. Isolation and characterization of a novel human paired-like homeodomain-containing transcription factor gene, VSX1, expressed in ocular tissues. Genomics **63**(2): 289–93. doi:10.1006/geno.1999.6093.

Shang, Z., Isaac, V.E., Li, H., Patel, L., Catron, K.M., Curran, T., Montelione, G.T., and Abate, C. 1994. Design of a “minimAl” homeodomain: the N-terminal arm modulates DNA binding affinity and stabilizes homeodomain structure. Proc. Natl. Acad. Sci. U. S. A. **91**(18): 8373–7. doi:10.1073/pnas.91.18.8373.

Shetty, R., Nuijts, R.M.M.A., Nanaiah, S.G., Anandula, V.R., Ghosh, A., Jayadev, C., Pahuja, N., Kumaramanickavel, G., and Nallathambi, J. 2015. Two novel missense substitutions in the VSX1 gene: Clinical and genetic analysis of families with Keratoconus from India. BMC Med. Genet. **16**(1): 1–11. doi:10.1186/s12881-015-0178-x.

Shi, Z., Jervis, D., Nickerson, P.E.B., and Chow, R.L. 2012. Requirement for the paired-like homeodomain transcription factor VSX1 in type 3a mouse retinal bipolar cell terminal differentiation. J. Comp. Neurol. **520**(1): 117–129. doi:10.1002/cne.22697.

Shi, Z., Trenholm, S., Zhu, M., Buddingh, S., Star, E.N., Awatramani, G.B., and Chow, R.L. 2011. Vsx1 Regulates Terminal Differentiation of Type 7 ON Bipolar Cells. J. Neurosci. **31**(37): 13118–13127. doi:10.1523/JNEUROSCI.2331-11.2011.

Sridhar, M.S. 2018. Anatomy of cornea and ocular surface. Indian J. Ophthalmol. **66**: 190–194. doi:10.4103/ijo.IJO.

Tang, Y.G., Picornell, Y., Su, X., and Li, X. 2008. Three VSX1 Gene Mutations, L159M, R166W, and H244R, Are Not Associated With Keratoconus. **27**(2): 189–192.

Tanwar, M., Kumar, M., Nayak, B., Pathak, D., Sharma, N., Titiyal, J.S., and Dada, R. 2010. VSX1 gene analysis in keratoconus. Mol. Vis. **16**(September): 2395–401. doi:257 [pii].

Torricelli, A.A.M., and Wilson, S.E. 2014. Cellular and extracellular matrix modulation of corneal stromal opacity. Exp. Eye Res. **129**: 151–160. Elsevier Ltd. doi:10.1016/j.exer.2014.09.013.

Valgaeren, H., Koppen, C., and Van Camp, G. 2017. A new perspective on the genetics of keratoconus: why have we not been more successful? Ophthalmic Genet. **39**(2): 1–17. Taylor & Francis. doi:10.1080/13816810.2017.1393831.

Valleix, S., Nedelec, B., Rigaudiere, F., Dighiero, P., Pouliquen, Y., Renard, G., Le Gargasson, J.F., and Delpech, M. 2006. H244R VSX1 is associated with selective cone on bipolar cell dysfunction and macular degeneration in a PPCD family. Investig. Ophthalmol. Vis. Sci. **47**(1): 48–54. doi:10.1167/iovs.05-0479.

Vincent, A.L., Jordan, C., Sheck, L., Niederer, R., Patel, D. V, and McGhee, C.N.J. 2013. Screening the visual system homeobox 1 gene in keratoconus and posterior polymorphous dystrophy cohorts identifies a novel variant. Mol. Vis. **19**(April): 852–60.

Wang, Y., Rabinowitz, Y.S., Rotter, J.I., and Yang, H. 2000. Genetic epidemiological study of keratoconus: Evidence for major gene determination. Am. J. Med. Genet. **93**(5): 403–409. doi:10.1002/1096-8628(20000828)93:5<403::AID-AJMG11>3.0.CO;2-A.

Watson, T., and Chow, R.L. 2011. Absence of Vsx1 expression in the normal and damaged mouse cornea. Mol. Vis. **17**(March): 737–44. Available from http://www.pubmedcentral.nih.gov/articlerender.fcgi?artid=3062518&tool=pmcentrez&rendertype=abstract.

Weiss, J.S., Møller, H.U., Aldave, A.J., Seitz, B., Bredrup, C., Kivelä, T., Munier, F.L., Rapuano, C.J., Nischal, K.K., Kim, E.K., Sutphin, J., Busin, M., Labbé, A., Kenyon, K.R., Kinoshita, S., and Lisch, W. 2015. IC3D Classification of Corneal Dystrophies—Edition 2. Cornea **34**(2): 117–159. doi:10.1097/ICO.0000000000000307.

Weissman, B.A., Ehrlich, M., Levenson, J.E., and Pettit, T.H. 1989. Four Cases of Keratoconus and Posterior Polymorphous Corneal Dystrophy. Optom. Vis. Sci. **66**(4): 243–246.

Weymouth, A.E., and Vingrys, A.J. 2008. Rodent electroretinography: Methods for extraction and interpretation of rod and cone responses. Prog. Retin. Eye Res. **27**(1): 1–44. doi:10.1016/j.preteyeres.2007.09.003.